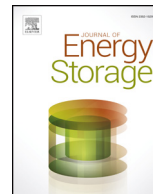




ELSEVIER

Contents lists available at ScienceDirect

Journal of Energy Storage

journal homepage: www.elsevier.com/locate/est

Capability study of dry gravity energy storage[☆]

C.D. Botha^{*}, M.J. Kamper

Stellenbosch University, South Africa



ARTICLE INFO

Keywords:

Renewable energy
Gravity storage
Electromechanical storage

ABSTRACT

The increasing penetration of intermittent renewable energy sources has renewed interest in energy storage methods and technologies. This paper describes a gravitational potential energy storage method. A review of current storage methods that make use of the principle of gravitational potential energy is done, with a comparison given in terms of power, energy rating and round trip efficiency. One of these gravitational energy storage methods, involving moving a solid mass vertically up and down, is further analysed in terms of energy storage capacity, energy and power density and the levelised cost of storage. Two different hoisting methods are discussed, the first of which is the traditional drum winder hoist and the second is a proposed, multi-piston hoist based on the use of linear electric machines. The two hoist methods produce storage systems with distinctly different properties and storage applications.

1. Introduction

With the increasing penetration of renewable energy sources (RESs), the need to manage the inherent intermittency of sources such as wind and solar power has also increased. While traditional energy systems are well equipped to handle variability in energy demand, the additional energy supply uncertainty introduced by the integration of large amounts of renewable energy will require new kinds of flexibility measures to ensure grid stability [1].

Studies show that RES penetration up to 30% can be adequately accommodated by improving operational practices [1–3], with several countries (e.g. Portugal, Ireland and Cyprus) generating between 20 and 30% from variable RESs without any additional storage [4]. However, as RESs continue to increase their share of generation responsibilities, the need to ensure adequate grid flexibility and reliability has renewed interest in technologies and strategies that can help mitigate the effects of RES [5].

One such technology, which can be especially useful in increasing the penetration of RESs, is energy storage [1,6]. The renewed interest in energy storage methods have led to an increase in the amount of research done, with the progress being well documented in various review papers [6–16]. The interest in and need for further development of energy storage systems, both technically and economically, is thus of great importance.

There are numerous ways to classify energy storage systems. Broadly, such systems can be classified by either the form of the

converted energy or the use of the storage, i.e. the service provided by the storage system [10]. The form of the storage can be divided into five main categories, namely chemical, electrochemical, electrical, mechanical and thermal energy storage [9].

Qualifying the storage methods by means of the service produces the three overarching categories described below [10,8] and summarised in Table 1.

- **Bulk Energy Storage** – Associated with services such as load shifting, providing spinning reserves and long-term storage, these systems have a stored energy range of 1 MWh–8 GWh and discharge times between 1 and 8 h.
- **Distributed Generation** – Storage systems better suited to applications such as peak shaving, regulation services to help correct short-term power imbalances and upgrade deferral. These systems are often deployed to reduce the load on the network, with a stored energy range of 0.05–8 MWh and discharge times between 30 min and 4 h.
- **Power Quality** – Generally systems that can respond very fast, they ensure end-user power quality and reliability by helping maintain voltage levels and transient stability. These systems have a stored energy range of 0.02–17 kWh and a discharge time of 1–30 s.

These definitions are purposely vague and even with them stated as above, technological advancement has resulted in systems that can provide multiple services [8], making classification more difficult.

[☆] This research did not receive any specific grant from funding agencies in the public, commercial, or not-for-profit sectors.

^{*} Corresponding author.

E-mail address: 17058945@sun.ac.za (C.D. Botha).

Table 1
Summary of storage categories based on the service provided.

Service category	Storage capacity	Discharge time
Bulk energy storage	0.001–8 GWh	1–8 h
Distributed generation	0.05–8 MWh	0.5–4 h
Power quality	0.02–17 kWh	1–30 s

Consequently, it is useful to evaluate any storage system by fundamental attributes. Some of these characteristics can be defined as follows [8,7]:

- **Energy storage capacity and duration** – Refers to the amount of energy that can be stored and the duration that said energy can be stored.
- **Energy/power density** – Energy density (Wh/m^3) is the energy stored per unit volume of the system and power density (W/m^3) is the output power per unit volume.
- **Lifetime** – The life span if the storage technology, measured in either years or total charge/discharge cycles.
- **Charge/discharge and response time** – The time needed to charge or discharge fully. Response time is the time needed to start providing rated power output.
- **Roundtrip efficiency** – Also called the AC-to-AC efficiency, this is defined as $\frac{\text{OutputEnergy}}{\text{InputEnergy}} * 100\%$, for one charge/discharge cycle.
- **Capital Cost** – The upfront costs of a storage technology, either per unit of power discharge or per unit of energy discharge.

Analysing any storage system therefore requires weighing up a number of the relevant characteristics and capabilities, as different renewable resources will have unique grid integration and service requirements depending on various details such as the type and location of the renewable source.

This paper focuses on gravity energy storage (GES), a subcategory of mechanical energy storage which includes traditional pumped hydroelectricity storage. Section 2 provides a review of the existing GES technology, Sections 3 and 4 presents an in-depth look at a proposed GES technology, with Sections 5 and 6 analysing two proposed hoisting methods. Lastly, some conclusions are given in Section 7.

2. Overview of existing gravitational energy storage methods

Using the gravitational potential energy of an object as a way to store energy is not a new idea. Pumped hydroelectric storage (PHES) is currently the most used storage method in the world, especially for long-term, large-scale storage [17,12]. There have been a number of variations on the traditional PHES layout, while recently work has been done on dry, i.e. waterless, forms of GES. The following two subsections provide an overview of systems in these subcategories.

2.1. Wet gravitational energy storage

The storage methods described below are variations on traditional pumped hydroelectricity storage.

PHES – Pumped hydroelectricity accounts for more than 99% of bulk storage capacity in the world [12] and as a result, PHES is the most mature large-scale energy storage method worldwide [7,17]. In most cases, PHES systems have two reservoirs, one higher and one lower. The system stores energy in the form of the potential energy of the water in the higher reservoir, to which the water is pumped during off-peak time. The water is released to the lower reservoir through turbines to generate electric power during periods of high demand.

Despite numerous advantages, such as scalability, long-term storage and a high round trip efficiency (between 65 and 87%) [7], PHES systems have some obvious disadvantages. As gravity on earth is a

relatively weak force, the energy density of the system is low, thus requiring a large variation in height or a large body of water to store a substantial amount of energy. Site selection criteria include sufficient water supply, correct topography, social acceptability and economical feasibility [17].

Underground PHES – In areas where the topography is not suitable for traditional PHES, underground PHES (UPHES) provides an attractive alternative [11]. In this case, the upper reservoir is placed above ground and the lower reservoir directly beneath it underground. Doing this ensures that a high vertical displacement is achievable without consuming a large surface area, allowing one to be constructed wherever there is low value ground. Similarly, some work has been done to explore the viability of the use of deep mines and open pit mines for UPHES [18,19]. The authors of [19] specifically propose UPHES for deep level gold mines in South Africa which can function as both a storage system and a way to purify the highly acidic and polluted water contained in flooded mines.

Piston-based PHES – Also called Piston-In-Cylinder electrical energy storage [6], it entails the use of water to lift a piston (any object with the required mass), thereby storing energy that can be released by letting the piston descend, pushing the water back through hydroelectric generators. This concept forms the basis for a trio of energy storage companies [20–22].

The Gravity Power Module (GPM) utilises a very large piston suspended in a deep, water-filled shaft and a return pipe connected to a pump-turbine [20], as illustrated in Fig. 1. When charging, water is pumped through the return pipe, lifting the piston up in the shaft. Discharging the system entails the piston moving downwards, thereby forcing the water back through the return pipe and turbine. The sizes under consideration can vary from a piston diameter of 30–100 m, a shaft depth of 500–1000 m and a piston length exactly half of the shaft length. The aim is to provide power and energy in the range of 40 MW/160 MWh to 1.6 GW/6.4 GWh [20]. Some research has also been conducted on this storage method, with the authors of [23][23a] presenting a system design and economic evaluation of a 5 MW/20 MWh GPM. The same authors also present the dynamic modelling of a GPM system in [24].

Both Heindl Energy [21] and EscoVale [22] have similar ideas, but larger in scale and with a different construction layout. Heindl Energy's system is called hydraulic hydro storage (HHS) [25] and EscoVale's system is called ground-breaking energy storage (GBES) [22,26]. The construction of both systems is achieved by excavating and reinforcing

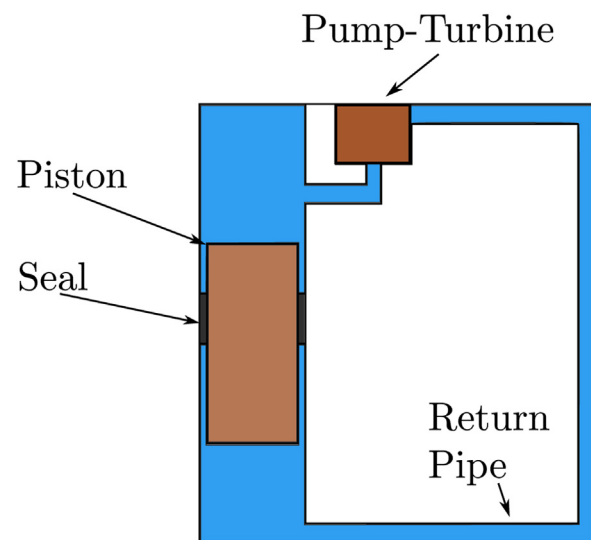


Fig. 1. A simplified illustration of the Gravity Power Module. The system is charged by pumping water to raise the piston and discharged by allowing the piston to descend, thereby pushing water through the turbine.

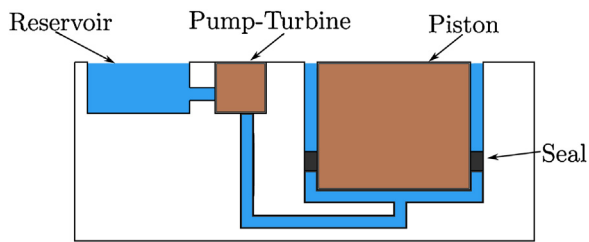


Fig. 2. A simplified illustration of the concept for both Heindl Energy and Escovale. The system is charged by pumping water from the reservoir to raise the piston and discharged by letting the piston descend, thereby pushing water through the turbine back into the reservoir.

an area to form a natural piston. The excavated portion is then connected to a return pipe and sealed to ensure there is no water leakage. A simplified diagram of this form of storage is given in Fig. 2. From here the operational principle is the same as for the GPM system. The proposed storage sizes range from 1 to 10 GWh [22,21,6]. These piston-based technologies all have the advantage of less rigorous topographical requirements than that of traditional PHES.

Underwater Ocean Storage Systems (UOSS) – This type of storage system is specifically designed to be used with a renewable energy plant floating offshore [27,28]. The storage system consists of a submerged vessel (e.g. a large tank or a set of pipes/cylinders in [27] or a hollow concrete sphere as in [28]), a reversible turbine coupled to the vessel and an electric cable system connecting the turbine to the generating unit (e.g. a floating PV plant or wind turbine). The submerged vessel is moored to the ocean floor and the water is pumped out of the vessel during the charging cycle and flows back into the vessel when discharging. The size of the storage system will be completely dependent on the generating unit, but the example given in [27] shows a vessel with a volume of 360 m^3 at a depth of 1000 m will be able to store 984 kWh at an efficiency of 90%, while [28] presented larger scale systems (in the area of a few GWh) with estimated efficiencies of 65–70% (Fig. 3).

2.2. Dry gravitational energy storage

The storage technologies described in this section all rely on the same operating principle as the previous section's storage methods, but do not require the use of water.

ARES – Advanced rail energy storage (ARES) LLC is a California-based technology development company dedicated to increasing the role of energy storage in the electrical grid [29,6]. The company has developed a rail-based, traction drive technology, ARES, that uses surplus renewable energy or low-cost electricity from the grid to move a mass, in the form of concrete blocks, uphill by rail road shuttles. The shuttles are then allowed to descend under gravity when the system is being discharged. The shuttles each weigh around 45–64 t and travel on

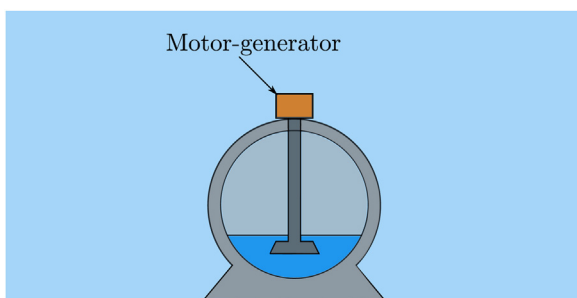


Fig. 3. A simplified illustration of a spherical UOSS, as given in [28]. The system is charged by pumping water out of the sphere, and discharged by letting the water flow back into the sphere.

a 16 km trail with a grade up 8.5% [6]. The system has a claimed efficiency of 78–80%, with no standby storage losses (i.e. no self-discharge) and a proposed system lifetime of 40 years. ARES LLC has a small pilot project that demonstrated the technology in Tehachapi, California [29] and is currently building the first commercial project in Nevada, a 50 MW, 12.5 MWh system, with a 9.3 km track at an average grade of 7.05% and a gross shuttle mass of 780 t.

Gravitricity – The concept behind the technology of Gravitricity is to vertically raise/lower a heavy mass down a shaft in the ground [30,31]. The stated plan is to build pistons with a mass up to 3000 t and use shafts that go as deep 1500 m [31], using either existing mine shafts or purposely built shafts. The mass is lifted with a system of guide cables, cables and winch systems, similar to the hoisting systems used in mines and cranes. Gravitricity claim an efficiency of around 80–90%, a response time of around 0.5 s, a 50-year design life and an output duration ranging from 15 min to 8 h.

An addition proposed by Gravitricity, is the use of a compressed air energy storage component. By sealing the shaft, the space can simultaneously be used as a pressure vessel for compressed air, potentially increasing the amount of energy stored by as much as a factor of three [31]. Gravitricity has received funding at the beginning of 2018 to build a 250 kWh prototype in South Africa [32,33].

Similar to Gravitricity, MGH Deep Sea Energy Storage [34] suggests raising and lowering the masses from a platform floating offshore, thus removing the need for shaft infrastructure. StratoSolar [35] proposes the same idea, with the masses being raised/lowered from a PV farm floating on buoyant platforms at an altitude of 20 km.

A summary of the important aspects of the above discussed storage methods is given in Table 2. UPHEs is not shown due to the similarity to traditional PHES. The power rating as well as the discharge time for these technologies are difficult to define properly, as they are highly context specific.

3. Modelling of a gravitational energy storage system

This section provides the modelling of a gravitational energy storage system. The focus is on the development of equations describing the energy storage capacity, the energy and power densities, the forces acting on the piston and providing an economic description of the system, with each aspect covered in its own subsection.

The idea behind the GES system is to store electrical energy by converting it to gravitational potential energy. The system is charged by lifting a certain mass and discharged when the mass is allowed to descend. An example of the GES system is given in Fig. 4.

3.1. Energy storage capacity

To analyse the energy storage capacity, the potential energy of the piston can be stated as

$$E = mgh, \quad (1)$$

where m is the mass in kg, g is the gravitational constant (9.81 m/s^2) and h is the height. Converting between Joule (J) and Watt-hour (Wh) is done as in (2).

$$1 \text{ kWh} = 3.6 \times 10^6 \text{ J} \quad (2)$$

Expanding on (1), the mass m can be written as ρV_p , where ρ is the density of the piston material and V_p is the volume of the piston. Assuming the piston takes the form of a cylinder as shown in Fig. 4, the mass can be written as

$$m = \rho \pi \left(\frac{d_p}{2}\right)^2 l_p, \quad (3)$$

where d_p is the piston diameter and l_p is the piston length. The stored energy, in Joule, can now be given as

Table 2
Summary of GES technologies.

Storage technology	Power rating	Energy rating	Discharge time	Life time (years)	Efficiency
PHES	1–5000 MW	1 MWh–20 GWh	1–24 h +	40–60	65–87%
GPM	40–1600 MW	1.6 GWh–6.4 GWh	1–4 h	40 +	75–80%
HHS	20–2750 MW	1 GWh–10 GWh	1–24 h +	40 +	80%
GBES	100 MW to multi-GW	Up to 20 GWh	24 h +	40 +	80%
UOSS	Up to a few GW	Up to a few GW	1–10 h	n/a	65–90%
ARES	100–3000 MW	Up to 6 GWh +	2–24 h	40 +	78–80%
Gravitricity	Up to 40 MW	Up to a few MWh	min–2 h	50 +	80–90%

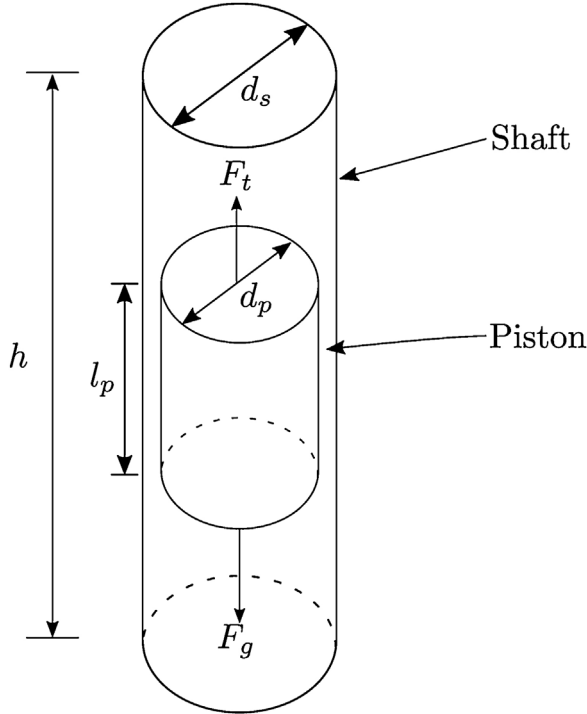


Fig. 4. A simplified illustration of the GES system.

$$E = \rho\pi\left(\frac{d_p}{2}\right)^2 l_p g h. \quad (4)$$

Using (2), the stored energy can be written in kWh as

$$S = 2.78 \times 10^{-7} \rho\pi\left(\frac{d_p}{2}\right)^2 l_p g h. \quad (5)$$

The energy density of the GES system, in kWh/m³, can be stated as

$$S_D = \frac{S}{V_s} \quad (6)$$

$$= \frac{2.78 \times 10^{-7} \rho\pi\left(\frac{d_p}{2}\right)^2 l_p g h}{\pi\left(\frac{d_s}{2}\right)^2 l_s}, \quad (7)$$

where the subscript *s* refers to the shaft. Assuming that the length of the shaft is the same as the height that the piston travels, i.e. $l_s = h$, and the piston diameter is roughly the same as the shaft diameter, i.e. $d_p \approx d_s$, (7) can be simplified to

$$S_D = 2.78 \times 10^{-7} \rho g l_p. \quad (8)$$

In the same manner, an equation for the power density of the GES system can be derived. This is given in (9) in kW/m³, where t_{dis} is the discharge time of the GES system in h.

$$P_D = \frac{\rho l_p g}{3.6 \times 10^6 t_{dis}} \quad (9)$$

From (8) and (9), an interesting quality of the GES system becomes apparent. Both the energy and power densities are dependant on the length of the piston and the density of the piston material. This property is true for any shape, as long as both the shaft and piston have the same shape.

3.2. Mathematical description of the resulting piston forces

To relate the storage capacity of the GES system with the capability of different hoisting methods, the force required to move the piston can be expressed with regards to the mass and acceleration of the piston. The force required to accelerate the piston from a standstill to a constant velocity can be written as

$$F_t = F_a + F_g = ma + mg, \quad (10)$$

where *a* is the acceleration, defined as $\frac{\Delta v}{\Delta t}$. Typical acceleration times for mining hoists are in the range of 0.5–0.75 m/s² [36,37]. When compared to the value of *g* (9.81 m/s²), the force necessary during the acceleration/deceleration could be as little as 5% higher than during steady-state discharge. This, in turn, points to the possibility of fast response times, as the discharge velocity of the GES tends to be slow.

As an example, if the GES system is located in a 2 km mining shaft and had a discharge time of 2 h (as given in Table 2 for Gravitricity), it would have a discharge velocity of $v_2 = 0.28$ m/s. Choosing an acceleration value of 0.5 m/s², this would yield a response time of $t = 0.56$ s, similar to what Gravitricity cites as being their system's response time [30,31].

3.3. Economic description of the piston

An important metric of any storage technology is the levelised cost of energy storage (LCOS). The LCOS provides a detailed calculation of the cost per stored unit of energy and can be used to compare the cost of one storage system with other storage systems that use different cost structures. The LCOS equation, given in [38], can be stated as

$$LCOS = \frac{CAPEX + \sum_{t=1}^{t=n} \frac{A_t}{(1+i)^t}}{\sum_{t=1}^{t=n} \frac{S_{out}}{(1+i)^t}}. \quad (11)$$

In (11), CAPEX is the upfront capital expenditure, and can be split into energy and power components, A_t is the annual cost of the storage system, summed over the storage system's lifetime and discounted at an interest rate *i*. The numerator is divided by the sum of the annual energy output, S_{out} , which is also discounted at the same interest rate.

The annual cost A_t of the storage system is given as [38]

$$A_t = COPEX + CAPEX_{re} + C_{el} S_{in} - R. \quad (12)$$

Here, COPEX is the operational cost, expressed as a fixed percentage of the CAPEX per year, $CAPEX_{re}$ is the replacement costs of specified system components and C_{el} is the cost of electrical energy (cost/kWh), multiplied by the input energy S_{in} to provide an estimate of the cost of electricity supply. At the end of the system's life, a recovery value *R* can be included.

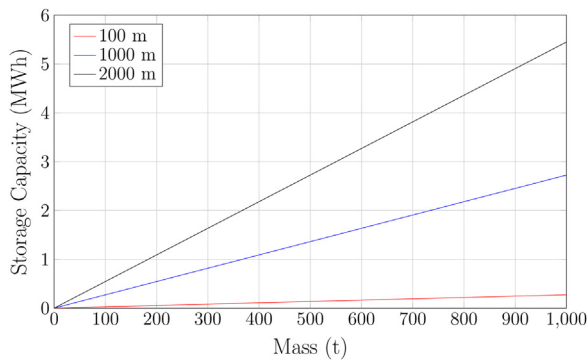


Fig. 5. Storage capacity described in terms of three relative system heights and mass.

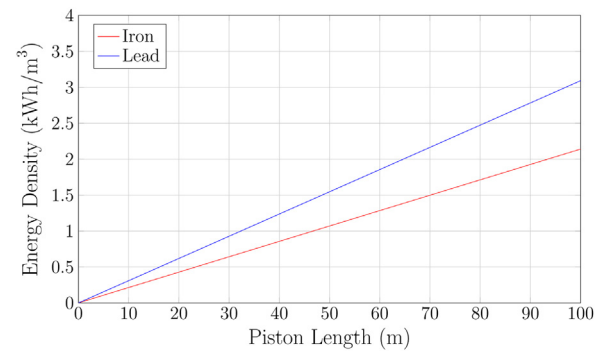


Fig. 6. Energy density of the GES system as it relates to the length of the piston.

The annual energy output S_{out} can be formulated as

$$S_{out} = DoD * n_{cycles} * (\eta S_{rated}), \tag{13}$$

where DoD is depth of discharge, n_{cycles} is the annual amount of charge/discharge cycles, S_{rated} is the system rated energy in kWh and η is the round trip efficiency.

4. GES performance capability

To illustrate the performance of the GES, this section uses the system modelling from the previous section to analyse the storage capacity of the GES, the energy and power densities that are possible using different piston materials as well as the potential LCOS of such a storage system. A discussion of the different piston materials is also done.

4.1. Storage capacity

Using (1) and (2), Fig. 5 relates the storage capacity of the GES as the piston mass increases for three chosen system heights, 100 m, 1000 m and 2000 m. This gives an indication of the amount of mass needed, as well as the system height, to achieve a few MWh of storage. At a height difference of 2000 m and a mass of 1000 t, which gives a storage capacity of 5.4 MWh, the storage capacity of the GES is lower than all of the gravity-based storage systems listed in Table 2.

4.2. Piston material

From (8) and (9) it can be seen that the choice of piston material has an effect on the energy and power density of the GES and thus the overall size of the storage system. This choice also has an effect on the cost of the system. Given in Table 3 are a few heavy metals that are commonly used in construction. The prices given are for the raw material, i.e. ore, and thus do not include the cost of transporting or processing [23][23a]. If these are taken into consideration, the material cost could be higher.

From Table 3, lead, copper and iron appear to be viable options based on their density and availability. However, when comparing the price per tonne of these materials, it is apparent that copper is not a

Table 3
Common construction material properties.

Material	Density (kg/m ³)	2017 World production (t) [39]	Price per t (€ ₂₀₁₇ /t) [40]
Aluminium	2712	60 million	1728
Copper	8940	19.7 million	5660
Iron	7850	1200 million	80
Lead	11340	4.7 million	2258

practical choice, given the price increase over iron (5580 €/t), with only a 13.9% increase in density. Lead and iron are chosen to help demonstrate the effect that the material density has on the energy density, power density and LCOS of the GES system.

4.3. Energy and power densities

Using (8), the energy density for varying piston lengths is shown in Fig. 6. A 100 m piston length may seem impractical, though this size is still smaller than suggested by some of the other piston-based PHEs systems [20,25,26,2323a]. This piston size can be realised by having multiple smaller pistons in the same shaft.

Fig. 6 demonstrates the GES system's low energy density, which is not surprising as earth's gravitational force is relatively weak, with low energy densities being a hallmark of gravity energy systems [6]. The choice of piston material has a small effect on the system's energy density, as the increase in energy density between iron and lead is only 30.7%. A comparison of the GES energy density with other storage systems, with values as presented in [41], is given in Table 4.

The power density, as given by (9), is shown in Fig. 7. Aside from the length of the piston and the piston material density, the power density is also dependent on the discharge time. The power density is plotted against discharge time, with the piston material as a second variable. The power density is shown for two piston lengths, 10 m and 100 m.

The power densities shown in Fig. 7 point to the optimal discharge time for the GES, regardless of piston material, being between 0 and 2 h. The difference in power density as a result of piston material is also small, as is the case for the energy density. A comparison of the power density values of the GES and other storage systems is given in Table 4. It should be noted that the minimum and maximum values of the GES are determined by piston lengths of 10 and 100 m, respectively, and will vary depending on the piston size and material.

The GES system has the same power and energy density characteristics as flow batteries and lends itself to power applications such

Table 4
Comparison of the power and energy density of selected storage systems.

Storage system	Energy density (kWh/m ³)	Power density (kW/m ³)
GES	0.2–3.1	0.03–30
PHEs	0.133–0.5	0.01–0.12
CAES	0.4–20	0.04–10
Flywheel	0.25–424	40–2000
Li-ion	94–500	56–800
Flow batteries		
VRB	10–30	2.5–33.4
ZnBr	5.2–70	3–8.5
PSB	10.8–60	1.35–4.16

GES – gravity energy storage; PHEs – pumped hydroelectricity storage; CAES – compressed air energy storage; VRB – vanadium redox battery; ZnBr – zinc bromine; PSB – polysulfide bromide.

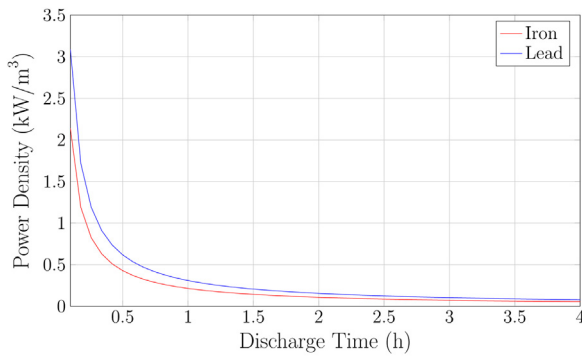
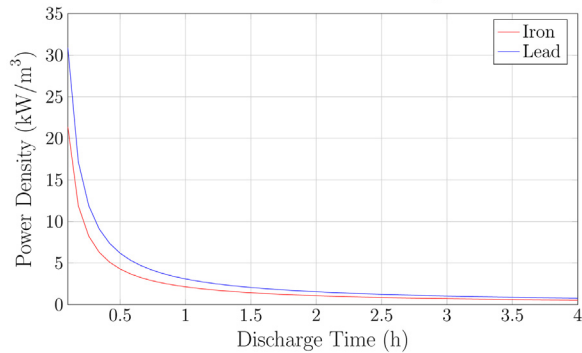
(a) Power density of a GES system with $l_p = 10$ m.(b) Power density of a GES system with $l_p = 100$ m.

Fig. 7. Power density of the GES for a piston length of (a) 10 m and (b) 100 m.

as those described by the distributed generations category in Table 1.

4.4. GES levelised cost of storage

The final metric used to describe the GES in the previous section is the LCOS. This is also the most difficult metric to accurately determine because of highly context specific costs. Examples of such specific costs are: the method of hoisting; how and where the system is installed (either in an already existing mineshaft, a mineshaft specifically excavated for the system, an above ground installation or a deep sea installation); and how the system is operated, e.g. the annual cycles has an effect on the operational and maintenance cost. Each situation will have differing costs, in capital investment cost, operational and maintenance costs as well as replacement costs. For the purposes of this study, it is assumed that a shaft is already available and the hoisting-specific costs, such as equipment and installation costs, are ignored.

A 10 MWh system is examined at two system heights, 100 m and 2000 m, to clearly demonstrate the effect that the piston material cost will have. The total mass required to store 10 MWh at these heights are 36697 and 1835 t, respectively.

Referring to the power densities in Fig. 7, a shorter discharge time would be optimal for a GES. This short discharge time will also take advantage of the high cyclability of the GES system, thus a discharge time of 30 min is chosen. The technical information of the system is given in Table 5, with the lifetime and η values based on the literature covered in Section 2.

The CAPEX term in (11) can be split into two terms, the energy-based investment cost and the power-based investment cost. The energy investment cost includes the components which can be described in $\$/\text{kWh}$. For this analysis, this comprises of the cost of the piston material. Using the average 2017 prices of iron and lead, the energy investment costs is given in Table 6.

The power investment cost consists of the power electronics, motor/generator unit and gearboxes, all of which are priced per kW. The

Table 5
Example GES system properties.

Property	Value
S_{rated}	10 MWh
P_{rated}	20 MW
Discharge time	30 min
DoD	1
η	85%
Lifetime	50 years

Table 6
List of piston material costs.

Material	Price per t ($\$_{2017}/\text{t}$)	$h = 100$ m ($\$/\text{kWh}$)	$h = 2000$ m ($\$/\text{kWh}$)
Iron	80	294	15
Lead	2258	8286	414

power electronics are taken as 84 $\$/\text{kW}$ [42]. The rest of the drive train is approximated as a three stage gearbox drive with a motor/generator unit, which can be approximated as 65 times the machine rating in kW [43]. Both of these costs are adjusted to reflect 2017 dollar values.

The operation and maintenance cost, COPEX, in (12) is difficult to estimate, as this value is likely to vary substantially between different GES systems. Gravitricity estimates the COPEX of their system as 0.5% of the CAPEX per year [44]. This is similar to the cost models for vertical shaft underground mines given [45], where the operational costs vary from 0.4 to 0.6% of the total capital costs, annually. Similar values are given in the economic comparison of vertical and decline shaft mining in [46]. As such, the COPEX value is taken as 0.5%.

The replacement cost, $CAPEX_{re}$, is approximated as a once-off expenditure halfway through the system's lifetime [44]. The cost of input electrical energy is taken as 0 $\$/\text{kWh}$ and the residual value, R , is ignored for the initial LCOS calculations. This is because of the difficulty in determining what value can be extracted from the piston material at the end of the system's life cycle, as well as the widely varying cost of input electrical energy, depending on where and when the system is used. The effect that both these input parameters have is investigated in the sensitivity analyses later in this section.

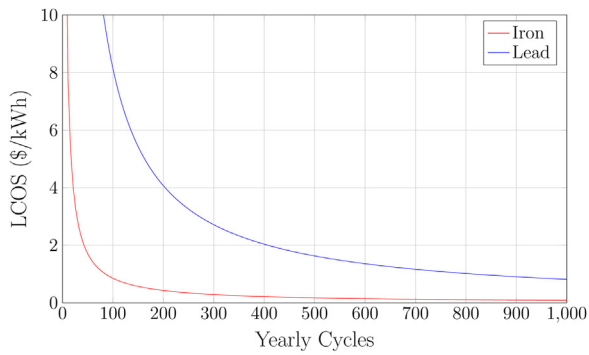
The LCOS values for the different systems are given in Fig. 8. The effect that the piston material has on the LCOS is pronounced at low annual cycles with a low system height, with an increase of $\approx 7\$/\text{kWh}$ between an iron-based and lead-based system. This difference becomes less significant as the annual cycles increase, becoming almost negligible in the 2000 m system. This can be ascribed to the fact that the piston material cost having a smaller share of the overall costs at 2000 m, with the power investment and replacement costs becoming more dominant.

The LCOS indicates that the GES system would be more economical at high yearly cycles, regardless of piston material or system height. This translates to shorter discharge times, which correlates well with the power densities shown in Fig. 7.

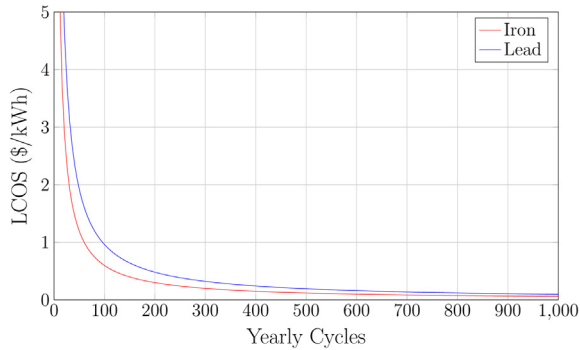
4.4.1. Sensitivity analyses

The LCOS is dependent on the accurate estimation of multiple input parameters. This subsection investigates the effect that the variation of CAPEX, COPEX, $CAPEX_{re}$ and η has on the estimated LCOS. The effect that the cost of input electrical energy and the recovery value has on the LCOS is also investigated.

To illustrate the effects that the chosen input parameters have on the LCOS, an iron-based GES system, at 100 m and 2000 m, and 730 annual cycles is taken as example. The cost share in terms of the energy investment, power investment, operating cost and replacement cost is given in Fig. 9. For both heights the power investment cost is the same



(a) The LCOS of a 100 m GES system.



(b) The LCOS of a 2000 m GES system.

Fig. 8. The LCOS of a GES system based at a system height of (a) 100 m and (b) 2000 m.

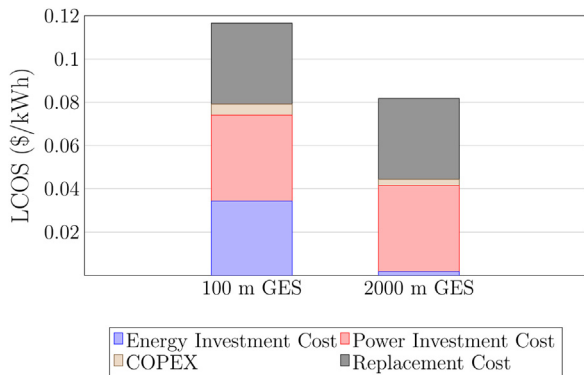
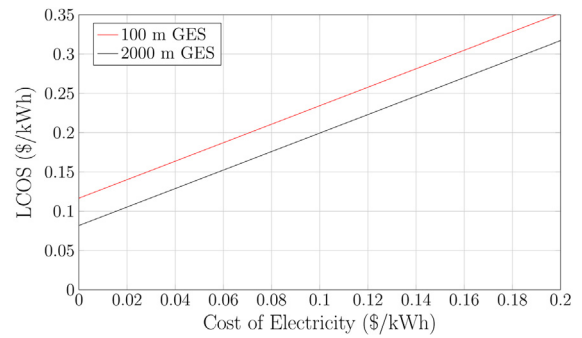


Fig. 9. The cost share components for a iron-based GES system at 730 annual cycles and a system height of 100 m and 2000 m.

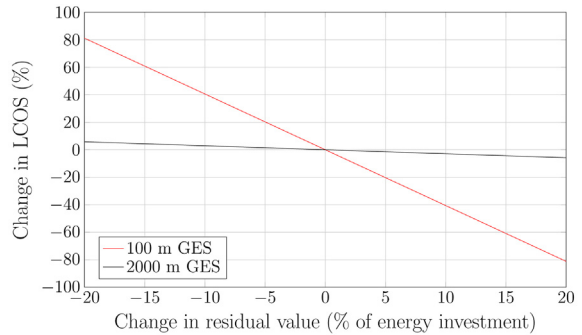
at 0.039\$/kWh, or 35% of the total LCOS at 100 m and 51% at 2000 m. The COPEX cost is less in the 2000 m system as the estimate is based on the total CAPEX, which is less for the 2000 m system. The replacement cost is also the same for both systems, as the estimate is based on the power investment cost.

Fig. 10 demonstrates the effect of adding the cost of electricity and a recovery value has on the LCOS. The cost of input electricity has a large effect on the projected LCOS, doubling the LCOS even at low electricity prices.

The change in recovery value extracted after the lifetime of a GES disproportionately affects the 100 m system. This is as expected, as the energy investment is higher for this system. To accurately estimate this term, the cost of extracting and recycling the piston material, as well as any cost with regards to the proper disposal of the power electronics, motor/generator unit and other hoisting-specific items should be taken into account. This could decrease the potential recovery value. Regardless, GES system with a large amount of piston material would



(a) The LCOS of an iron-based GES with a varying electricity cost.



(b) The change in LCOS of an iron-based GES system with varying recovery value, R .

Fig. 10. The effect on the LCOS of an iron-based GES of (a) the cost of input electrical energy and (b) the recovery value.

likely be able to recuperate a significant amount of money through the recycling of the piston material.

Fig. 11 shows the sensitivity analyses for the change in CAPEX, COPEX, CAPEX_{re} and η . The long lifetime of the GES system and high annual cycles mitigate the effect of a change in initial investment, with only 16% change in the LCOS for a change of 20% in CAPEX. The variation of COPEX has a smaller effect on the LCOS, requiring a change of 100% for a difference of 4% in the estimated LCOS. The change in CAPEX_{RE} has a large effect in the LCOS as it is based on the power investment, which has the largest cost share of the components. This explains why the change in LCOS for the 2000 m system is higher than the change for the 100 m system, as the power investment cost share is much larger. This indicates that it might be prudent to invest more heavily in the maintenance of the GES system, therefore ensuring that the least amount of replacements is needed. The effect that the system efficiency has is similar to the replacement cost. This is as expected, as the efficiency dictates how much usable energy is produced.

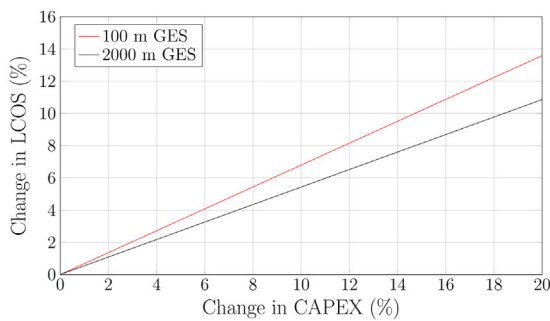
4.5. Discussion

This section covered the performance of the GES, demonstrated in terms of the storage capacity, energy and power density and the LCOS.

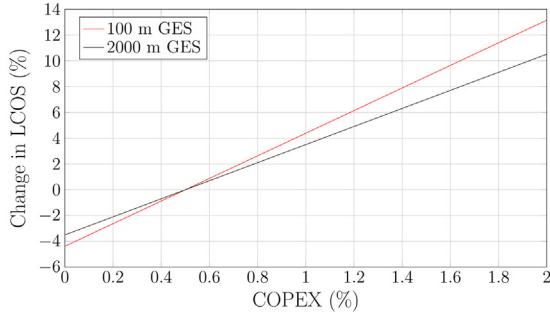
The storage capacity is limited by both the achievable system height and the amount of mass that can be hoisted, meaning that it can not readily achieve the high energy storage values (100 MWh +) of the other gravitational energy based storage systems.

The energy and power densities of the GES system is higher than traditional PHES, as expected, and is similar to the values for VRB and ZnBr batteries. The low energy density, paired with the short discharge times required to achieve some of the higher power densities, indicates that the GES is better suited for high power services, such as those described by the distributed generation in Table 1.

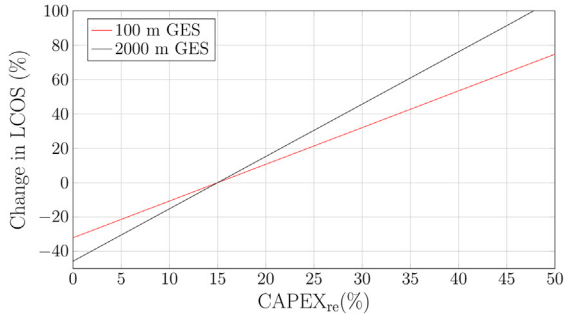
The choice of piston material does not have enough of an effect on the energy and power density values to justify the cost of the higher



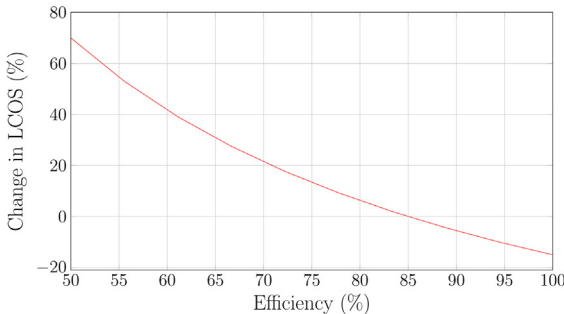
(a) The change in LCOS of an iron-based GES system with a varying CAPEX.



(b) The change in LCOS of an iron-based GES system with a varying COPEX.



(c) The change in LCOS of an iron-based GES system with a varying CAPEX_{re}.



(d) The change in LCOS of an iron-based GES system with a varying η .

Fig. 11. Sensitivity analyses for the LCOS of an iron-based GES system at 100 m and 2000 m.

density materials, thus iron is the ideal piston material. The LCOS, while rudimentary, indicates that higher annual cycles makes the GES more economically viable. Higher annual cycles directly equates to shorter discharge times, further emphasizing that the GES is well suited for distributed generation services such as frequency response.

It must be taken into consideration that the LCOS is done on the assumption that a shaft already exists. This is also the assumption made

by Gravitricity in their LCOS calculations in [44]. The cost of shaft excavation is likely to increase the capital costs considerably, with cost estimates of shaft development around 15,980\$/m [46]. A more detailed LCOS is needed to fully determine the economic feasibility of the GES. Such an economic evaluation needs to include the cost of hoisting specific equipments such as drum winders, wire ropes and equipment needed for the installation as well as a detailed look at the operational and maintenance costs of each component of the GES system. The change in COPEX with system height, piston mass and annual cycles should be investigated, as this could markedly affect the projected LCOS.

The following two sections investigate two specific hoisting methods. The first method, discussed in Section 5, is the conventional mine hoisting system. This is a very mature system. The second hoisting method is discussed in Section 6 and entails the use of linear electric machines as hoisting method.

5. Wire rope hoisting system

The first hoisting system under consideration is a conventional wire rope hoisting system, e.g. such as those used in elevators, mines and shipyards. These hoisting systems consist of mature technologies, making such a system an attractive option for the GES. The major components in a hoisting system are the winder drum and ropes, bearings, gearing, brakes, drive motor, power conversion and the hoist control system [45]. Wire rope hoisting systems commonly fall into two categories, drum or friction hoists. In a drum hoist system, the rope is connected, wound and stored on a drum, whereas in a friction hoist the rope only passes over the drum and is connected to a counterweight. For the GES system, only the drum hoist is applicable and is thus the focus of the rest of the section.

5.1. Wire rope hoist modelling

The capacity of a wire rope hoisting system is ultimately limited by the load that the wire rope can handle. The mechanical parts, e.g. the drum and the brake, are sized to match the rope loading, after which the electrical parts, e.g. the machine, gearbox and power electronics, are sized to match the torque and speed requirements of the mechanical parts [45]. The first part of this analysis therefore addresses the choice of wire rope and drum size.

A standard wire rope is constructed by twisting many small wires together to form a strand, with typical numbers of 7, 19 or 37 small wires per strand [47]. These strands are then twisted about a core, with the number of strands generally being six or eight [47,48], to form the wire rope. This rope is now flexible enough to wind around drums and sheaves. The wire rope diameter determines how large the drum diameter, d_{dr} , has to be, with the exact factor usually dependent on the type of wire rope used. A 6×7 wire rope will be less flexible than a 6×37 wire rope and thus require a bigger winder drum or sheave. Some properties of common wire rope constructions are given in Table 7, where d_r represents the wire rope diameter.

The factors by which the winder drum diameter has to be larger than the wire rope diameter given in Table 7 are only guidelines, with each wire rope manufacturer providing their own sizing, while different industries also have its own standards. In the mining industry, the drum

Table 7
Common wire rope sizes and properties [48].

Wire rope	Approximate mass (kg/m)	Area of metal (mm ²)	Minimum drum diameter (mm)
6×7	$3.45 \times 10^{-3} d_r^2$	$0.38d_r^2$	$42d_r$
6×19	$3.68 \times 10^{-3} d_r^2$	$0.4d_r^2$	$30d_r$
6×37	$3.57 \times 10^{-3} d_r^2$	$0.4d_r^2$	$18d_r$

diameter is generally larger by a factor of 70 for a standard wire rope [37] and given the similarity between mine hoisting systems and the GES system, a factor of 70 will be used when determining the drum size.

The initial wire rope selection is based on the three requirements [48]: the wire rope tensile strength, resistance to bending fatigue and abrasion resistance. Normally, a wire rope diameter is determined for each of these categories and the largest result is taken as the wire rope diameter. Given the relatively large d_{dr} to d_r ratio used and the very large amount of mass being hoisted, the resistance to bending fatigue is assumed to produce a smaller diameter than the required diameter based on the tensile strength would. Abrasive wear is less of a problem in vertical shafts [45], however, the abrasion resistance of a wire rope can be increased by selecting ropes with thicker wires, e.g. a 6×7 rope, or increasing the factor of safety when determining the wire rope diameter. It is thus assumed that the largest required diameter is produced by the wire rope tensile strength.

The tensile stress of a wire rope can be calculated by [47]

$$\sigma_t = \frac{F_{t1}}{A_{rope}}, \tag{14}$$

where σ_t is the tensile stress in N/mm^2 , F_{t1} is the resultant tensile force on the wire rope in N, and A_{rope} is the effective area of the wires in the rope as given in Table 7. The components that can be included in the tensile force are:

- The mass to be lifted;
- the mass of the wire rope at its longest;
- the acceleration and deceleration forces;
- any frictional resistance that needs to be overcome.

While the mass of the piston and the acceleration/deceleration forces are already taken into account in F_t in (10), the mass of the wire rope still needs to be taken into account. This can be done by approximating the mass of the wire rope as in Table 7 and multiplying it by the total length of the rope. The frictional forces can be approximated as 2.5% of the mass of the conveyance and 10% of the rope mass [45]. Thus, F_{t1} can be stated as

$$F_{t1} = \left[\frac{F_t}{N_r} + m_{rope} L_{rope} g + F_{friction} \right] * N_s, \tag{15}$$

where N_s is the safety factor, defined as the factor that the maximum tensile stress has to be higher than the required loading of the rope, and N_r is the number of wire ropes supporting the piston mass. The safety factor can be stated as [45]:

- For wire rope lengths of less than 914 m: $7 - 0.0033 * L$, where L is the length of the rope;
- for wire rope lengths of more than 914 m: 4.

For the purposes of this study, an average safety factor of 5 is assumed. After determining the rope diameter from (14), the drum velocity, in r/min, can be calculated using

$$n_{dr} = \frac{30v}{\frac{d_{dr}}{2}\pi}, \tag{16}$$

where v is equal to v_2 . Similarly, the drive train torque required to move the mass is given by

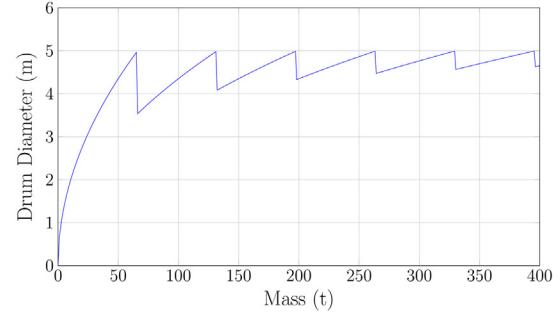
$$\tau = F_{t1} \frac{d_{dr}}{2}. \tag{17}$$

Lastly, the drive train power can be calculated by

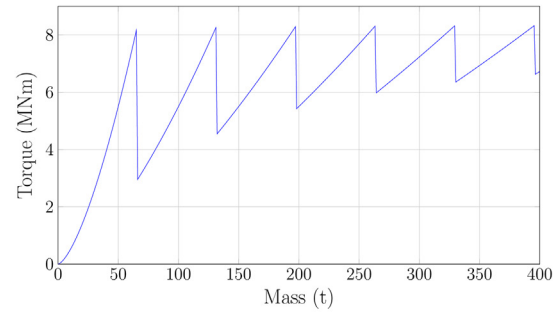
$$P = \left(\frac{n_{dr}}{30/\pi} \right) \tau. \tag{18}$$

Table 8
Wire rope system design specifications.

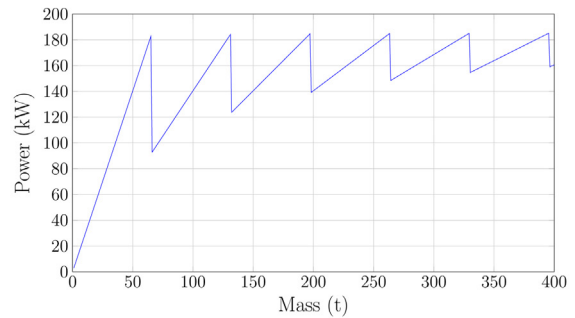
	h (m)	Discharge Time (h)	v_2 (m/s)	Wire Rope	Tensile strength (N/mm ²)
System 1	100	0.5	0.055	6×7	1770
System 2	2000	0.5	1.11	6×7	1770



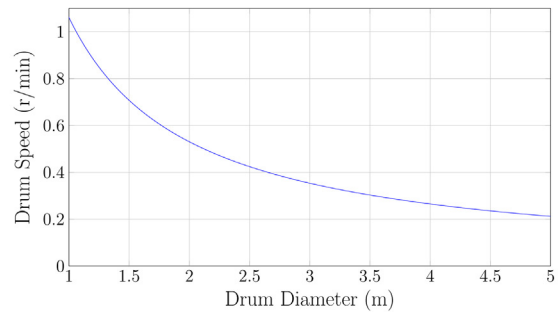
(a) Drum diameter versus piston mass. Each downward jump indicates the addition of a wire rope to the system.



(b) Torque per drum versus piston mass.

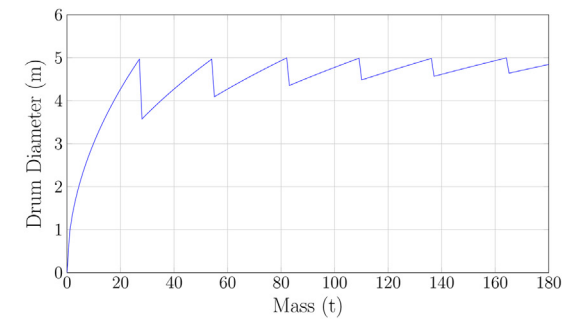


(c) Power per drum versus piston mass.

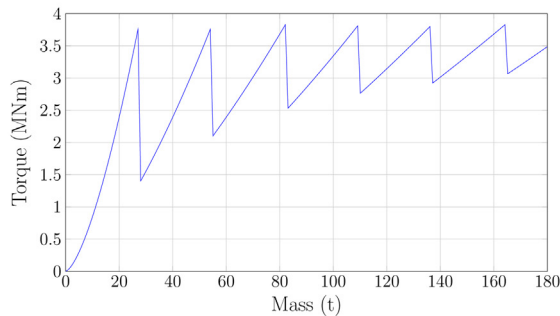


(d) Drum speed in r/min as the drum diameter increases.

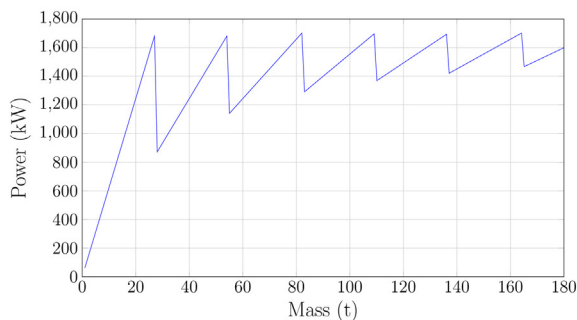
Fig. 12. Characteristics of a 100 m wire rope hoisting system. (a) Drum diameter, (b) torque per drum, (c) the power per drum, and (d) drum speed in r/min.



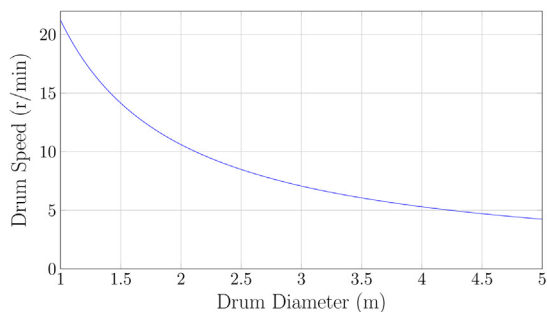
(a) Drum diameter versus piston mass. Each downward jump indicates the addition of a wire rope to the system.



(b) Torque per drum versus piston mass.



(c) Power per drum versus piston mass.



(d) Drum speed in r/min as the drum diameter increases.

Fig. 13. Characteristics of a 2000 m wire rope hoisting system. (a) Drum diameter, (b) torque per drum, (c) the power per drum, and (d) drum speed in r/min.

5.2. Wire rope hoist capacity

Using the above equations, two example systems, given in Table 8, are analysed. The system heights, while extreme, are chosen as a way to demonstrate the effect the system height has on the hoisting capacity. The discharge time is the same as used for the LCOS calculations in Section 4, while the choice of wire rope tensile strength is a commercially available value. A limit of 5 m is placed on the size of the drum

diameter and the total number of drums is limited to six. Figs. 12 and 13 show the drum diameter, drive train torque and power as well as the drum velocity.

The effect of the rope mass can be seen from Figs. 12 and 13 (a), as the achievable piston mass is a lot less in the 2000 m system than the 100 m. However, from (1), to achieve the same energy storage, a system with a 100 m height difference will require 20 times as much piston weight as a system with a 2000 m height difference.

The 100 m system also has a slower rotational speed and a larger torque requirement. This is likely to result in a larger, more complex drive train, as larger torque values usually result in a larger machine and the low rotational velocity needs to be stepped up by some form of gearbox. This increases the cost of the system. However, when compared to the 2000 m system, the 100 m system has a lot less wire rope, which may be able to mitigate the increased drive train complexity and cost.

5.3. Drive train technology

The slow rotational velocity of the winder drums shown in Figs. 12 and 13 (d), along with the high torque requirement, means a specialised drive train is needed to operate and drive the drums. This drive train consists of an electric machine and a gearbox of some form, similar to a wind turbine's drive train. While this can be realised in numerous ways, one of the most attractive options is a drive train utilising a magnetic gearbox or magnetically geared machine. This produces a highly efficient drive train, which is key to ensuring a high round trip efficiency. Most magnetic gearboxes have high efficiencies, between 80 and 99% [49–51] as well as high torque densities [52] and high gear ratios [53].

With regards to the machine, a conventional permanent magnet synchronous machine (PMSM) can be designed, such as the 79.5 kNm, 500 kW, 60 r/min presented in [54]. However, a specific PM machine topology, called the pseudo direct-drive (PDD) machine [55], appears to be extremely well suited to an application such as this. The PDD machine takes advantage of the properties of a magnetic gear and combine them with the high torque density of a conventional PM machine. The result is a machine designed for high-torque, low-speed operation. A design example of this machine is given in [56], where the authors design a 15 MW, 100 r/min, 1.43 MNm PDD machine.

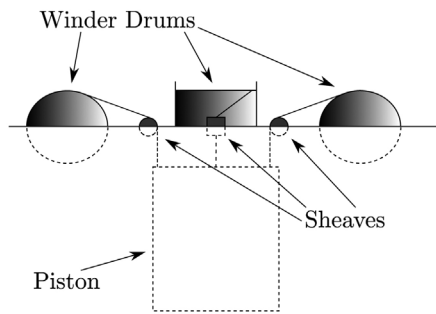
This technology is also commercially available, with Magnomatics [51] offering specially designed PDD machines which have an operating limit of anywhere from a few kW to a few MWs, a speed range of 10–1000 r/min, providing torque in the range of 1 kNm to 5 MNm and a claimed efficiency of above 97%. Magnomatics also does work on magnetic gearboxes, claiming they have a rated efficiency of 99%.

This brief review of options, while far from comprehensive, serves to demonstrate the feasibility of the wire rope hoisting system. It also indicates that it would be possible to have a high round trip efficiency.

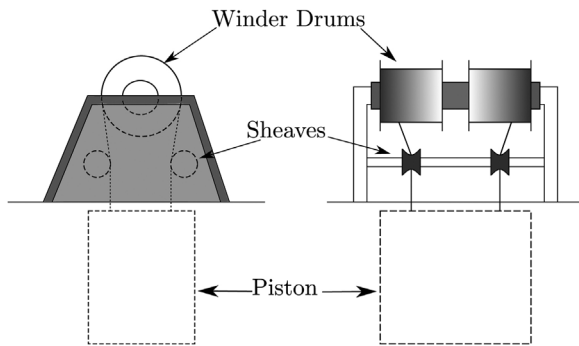
5.4. Practical hoist system implementation

As for the practical implementation, e.g. the placement of the winder drums, of such a wire rope hoisting system, there are numerous ways to accomplish this. Each will have its own advantages and disadvantages, and Fig. 14 displays two possible installations.

The first is a modified version of a conventional mine hoist and similar to the system proposed by Gravitricity for their prototype [30]. The example shown here represents a four drum system, though this can be adjusted as necessary. Such a system is well-suited for use in existing mine shafts and other systems where there is a large height difference. This is because of the available space around the shaft, which provides ample space for the very large drums, both in width and diameter, that are needed to store wire ropes with large lengths. If, for example, a drum diameter of 5 m is assumed, the wire rope diameter is 71 mm, with one turn of the drum storing the equivalent of 15.7 m of rope. To fully store the rope on the drum requires 128 turns. If the rope



(a) The conventional wire rope set up using a mineshaft, shown here as a four drum system.



(b) A wire rope hoisting system with the drum hosted in the headframe directly above the piston.

Fig. 14. Two different practical implementations of a wire rope hoisting system.

is stored in five layers, the drum needs to be close to 2 m wide. Ropes can be layered up to 15 times on a single drum [45], however this much layering would reduce the rope lifetime significantly and as such the trade-off between drum width and rope lifetime needs to be considered carefully.

The second set up is adjusted from a mining friction hoist [45], with the drum located on a headframe directly above the piston. While the example shown here has two drums, this can also be extended or reduced as needed. As an example, if the 100 m system is considered, the same 5 m diameter drum requires 7 turns to fully store the rope. This gives a drum width of 0.5 m, which is well-suited to a situation where there are multiple smaller systems built above ground and placed next to each other, as it allows for less space to be consumed per drum.

The actual piston size is completely independent of the hoisting capability of a wire rope hoist, and can be built to fit the specific use case. In the case where a mine shaft is used, which generally have a diameter of 10 m, the piston can be shaped so as to fit the shaft as a large disk, or be shaped as a smaller, narrower cylinder. Taking, for example, a 2000 m system with four winder drums which can hoist a total mass of 110 t. Assuming the piston is made of iron, this produces a piston with a total volume of 14 m^3 . If the piston diameter is roughly the same as a mine shaft, the piston would have a diameter of 10 m and a length of 0.178 m. This produces a GES system with a storage capacity of 600 kWh, an energy density of 0.0038 kWh/m^3 and a power density of 0.0076 kW/m^3 .

Considering the 100 m system and the set up shown in Fig. 14 as another example. Based on the larger torque requirements and allowing for the placement of the drive train, the number of drums are limited to two. This would allow a piston mass of about 200 t. Again assuming the piston material is iron, the total space consumed by the drums would likely be a circle with a radius of 5 m, similar to the winder drums. If the piston is that same diameter, then it would have a length of 1.3 m. The system specifications is given in Table 9, showing the low energy

Table 9

Example values of a wire rope hoisting system using the above mentioned hoisting set ups.

	h (m)	Energy storage (kWh)	Energy density (kWh/m^3)	Power density (kW/m^3)
System 1	100	54.64	0.028	0.056
System 2	2000	600	0.0038	0.0076

storage capacity that is the result of the limits placed by the wire ropes on the piston mass.

5.5. Discussion

A proper wire rope hoisting system design has to take into account a host of variables, such as discharge time, infrastructure, wire rope selection, drive train design, system height, storage capacity, number of drums, etc. This makes the design a multi-variable problem, with no one optimal solution. The preceding section chose two extreme height differences to illustrate how much wire rope systems are affected by the mass of the wire rope itself as well as provide some reference values in terms of storage capacity, energy and power densities for a practical implementation of a wire rope hoist.

Though only one type of wire rope construction (6×7) and tensile strength (1770 N/mm^2) is considered in this section, there are more options available, both commercially and specially built. This allows for greater freedom in the design process, as the selection of wire rope will go a long way in determining the minimum drum diameter and safety factor. Specially designed and built wire ropes have the potential to increase the possible piston mass, which is needed if the claimed piston masses of up to 3000 t by Gravitricity [31] are to be achieved. Similarly, it is possible to decrease the required tensile strength of the wire rope through the use of pulleys as is common in crane hoists applications.

The system examples shown here do not include shaft guides, which keep the piston in the proper position. These guides can be made of wood, steel or other wire ropes [45] and adds to the cost and complexity of the system, however does not affect the piston mass.

The type of drive train as well as the placement thereof also allows for a considerable degree of freedom. A standard set up with a gearbox and machine connected to the drum, is the most commercially mature option. Using machine technology such as the PDD means a direct drive is also a possibility, while the machine could potentially be installed inside the drum, thus freeing up more space around the drum. The machine and drum could potentially be placed on the piston itself, thereby contributing to the mass of the piston and lessening the total material needed for the piston.

The hoisting system can be applied in a variety of situations, such as in an abandoned mine shaft, specially built above ground structures, on a barge-like system floating on the ocean [34] or a platform floating in the air [35]. The wire rope hoist has some clear limits, but allows for a large variety of applications, ranging from smaller units built above ground, where multiple GES systems can be placed next to each other to form a beehive-like structure to large, single shaft GES systems placed in existing mines.

The effect that a wire rope hoisting system will have on the LCOS needs to be considered carefully. The equipment costs could significantly increase the initial capital costs, as indicated by the up to 50% share of capital cost of the mine cost model given in [45]. Wire ropes require in-use lubrication to ensure a long lifetime and have to be periodically inspected to ensure that fatigue is noticed before rope failure. Wire ropes and drum winders have an approximate cycling life, and would need replacing during the lifetime of the GES system. The same applies to the shaft guides, mechanical brakes and gearboxes. As indicated by the sensitivity analyses in Section 4, replacement cost has a significant impact on the LCOS of a GES system. All these factors

increase the operational and maintenance cost of the system.

6. Linear electric machine hoist

In the wire rope hoist, the gravitational potential energy of the piston, and its inherent linear motion, is converted to and from electrical energy by rotary machines through the indirect method of wire ropes, winder drums and gearboxes. The hoisting system described in this section proposes the use of linear electric machines (LM), which can directly convert the linear motion of the piston to and from electrical energy. Magnetically levitated (MAGLEV) trains, generators for wave energy conversion and ropeless elevators are some examples of the use of LMs [57–60]. LMs also do not require the use of wire ropes, a limiting factor of the previous hoisting method. They do, however, require application specific topologies and design and power electronics to control [57].

6.1. System description

LMs can be obtained by ‘cutting and rolling out’ the corresponding rotary machine [58] and can be classified as either flat or tubular in shape [59]. An example of a doubly salient, single-sided LM is given in Fig. 15.

As indicated in Fig. 15, the segment with the armature winding is referred to as the primary [58]. The second segment is referred to as the secondary or the translator [58], the rotor in rotary machines, and in this example only consists of the laminated steel. Numerous topologies exist with any combination of permanent magnets and windings on the primary, secondary or both [58,60].

The hoisting system can best be imagined as similar to a ropeless elevator [59,61–68,65,69,70], and an example with two single-sided LMs is shown in Fig. 16.

Since the secondary has to span the length of the system, it is imperative that it only consists of the laminated steel, and all the active parts are situated on the primary.

Fig. 17 provides a closer look at the two-sided piston example from Fig. 16, without the armature windings. Indicated on the figure are four linear guides. These guides can consist of mechanical parts, e.g. through linear bearings, although this will increase the maintenance of the system and decrease the overall efficiency due to the friction caused by the contact between the bearing and the guideway. Another option is the use of electromagnetic guides [65,71,72]. These consist of omega-shaped actuators, with permanent magnets and coils, around a steel guide rail and can be used to manipulate the attraction forces between the actuator and the guide rail. Using such a guideway, however, requires additional power electronics to control the omega-shaped actuator, thereby increasing the complexity and cost of the system.

Two other aspects, which are not indicated in Fig. 17, are the power supply and brakes. Since all the active material is on the short primary, located on the piston, it has to be supplied with electric power. This can be achieved in numerous ways, the simplest being the use of pantographs as in electric trains and trams. This is already an established technology and is simple to implement. Another attractive option is the use of the contactless power transmission method developed alongside

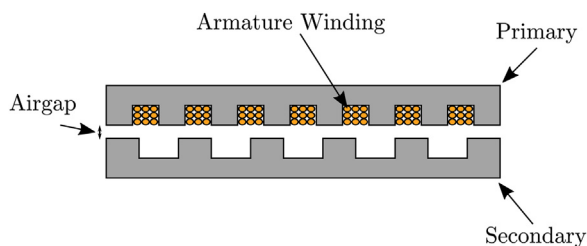


Fig. 15. An example of a flat, single-sided linear electric machine.

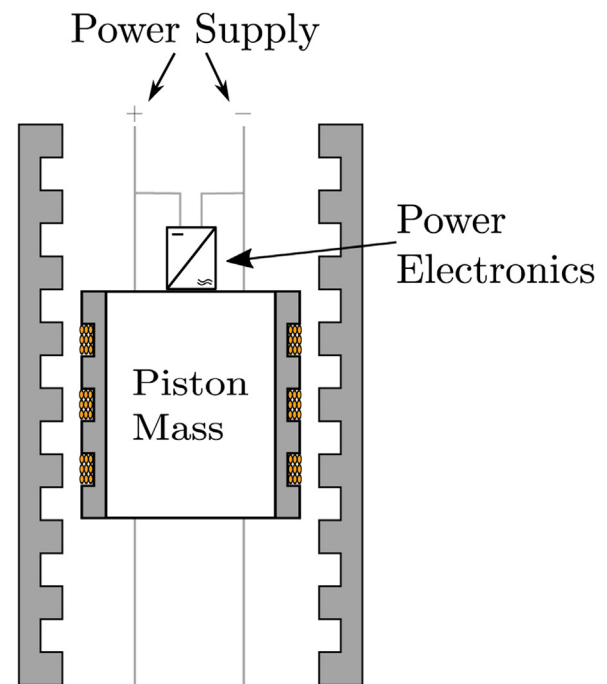


Fig. 16. An example of an LM-based GES system.

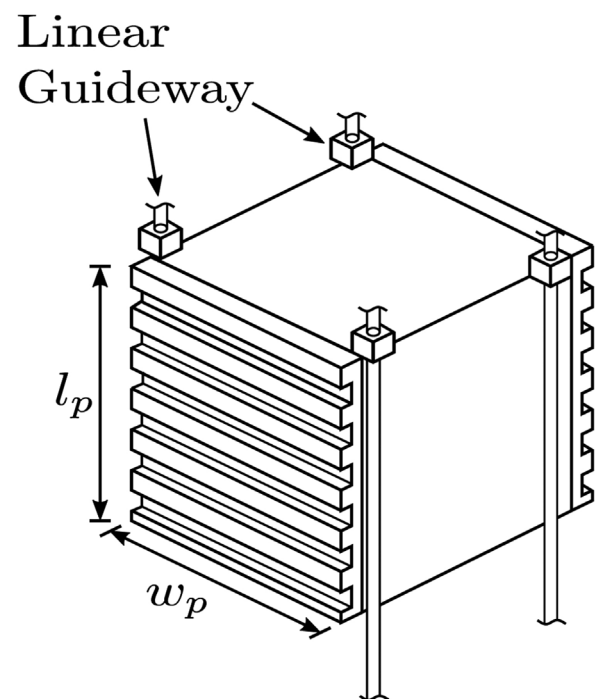


Fig. 17. An example piston, without the armature winding, for an LM-based GES system.

the omega-shaped actuator in [65,71,72], thereby combining both the guideway and power supply within one unit. Similar work has been done on the wireless power transfer systems for roadway powered electric vehicles [73], although both of these methods add more complexity to the system.

The braking system, which is especially important in case of a complete power failure, also presents a few options. Here the simplest method is again the traditional mechanical brakes, such as the friction brakes, usually installed on the drums of mine hoists and elevators [59,45]. They can be installed on the guideways, secured to the piston.

The example given in Figs. 16 and 17 relies on the use of a two-sided LM and a rectangular shaped piston. This allows for a simple illustration of the system and discussion of the necessary components of an LM-based hoist. However, in principle, the concept can be applied to any piston shape and the final choice of shape involves a trade-off between air gap area and practicality.

6.2. Sizing of linear electric machine hoist

Sizing linear electric machines is often done using air gap shear stress, which can be calculated as

$$\sigma = F/A, \quad (19)$$

where F is F_t and A is the effective air gap area. The shear stress provides a convenient way to relate the size of the electrical machine and the mass that can be hoisted, as well as provide a suitable criterion by which the numerous LM topologies can be compared.

If a tubular piston is assumed, then the area, A , can be defined as $2\pi(\frac{d_p}{2})l_p$. Using (10) to expand (19) results in

$$\begin{aligned} \sigma &= \frac{ma + F_g}{2\pi\frac{d_p}{2}l_p} \\ &= \frac{\rho\pi(\frac{d_p}{2})^2l_p a}{2\pi\frac{d_p}{2}l_p} + \frac{\rho\pi(\frac{d_p}{2})^2l_p g}{2\pi\frac{d_p}{2}l_p} \\ &= \frac{1}{2}\rho\left(\frac{d_p}{2}\right)a + \frac{1}{2}\rho\left(\frac{d_p}{2}\right)g \\ &= \frac{1}{2}\rho\left(\frac{d_p}{2}\right)(a + g) \\ &\approx \frac{1}{2}\rho\left(\frac{d_p}{2}\right)g \end{aligned} \quad (20)$$

If a four-sided piston is assumed, the area can be defined as $4w_p l_p$, where w_p is the width of the piston. Following the same derivation process as for the tubular shape, the shear stress equation for this shape is given by

$$\begin{aligned} \sigma &= \frac{1}{4}\rho w_p (a + g) \\ &\approx \frac{1}{4}\rho w_p g. \end{aligned} \quad (21)$$

This expanded equation for the shear stress reveals that its value is independent of the piston length, as long as the machine length is equal to the piston length.

6.3. Linear electric machine technology

As mentioned in the system description, a LM can be classified by shape, i.e. flat or tubular. Similarly, the LM can be classified as according to its topology. Two main classifications are the linear induction machine (LIM) and linear synchronous machine (LSM) [58].

Due to the inherently large air gap of LIMs, they suffer from low power factor and force density, i.e. shear force [58]. The secondary consists of two materials, a electric conduction layer (usually aluminium or copper) and a magnetic layer of mild ferromagnetic steel [58,57]. The magnetic field generated by the primary induces an eddy current in the solid secondary, lowering the machine efficiency [58]. Combined, these characteristics make a LIM unsuitable for use in the low velocity GES system.

LSMs have higher shear force, efficiency and power factor, but they are generally more expensive to manufacture due to the higher amount of active material used [58]. LSMs typically have a σ value in the range of 20–40 kN/m² [74,75] and can achieve an efficiency of 90% or more [74]. There are various methods of classifying LSMs, although for the purposes of this paper, they can be classified in two categories, i.e. electrically excited and PM LSMs.

Electrically excited LSMs have windings on both the primary and secondary and has received some attention for use in mine hoisting systems [76–78]. However, the windings on the secondary make them

inapplicable for use in a GES system.

The PM LSM may have PMs on either the primary, secondary or both, and have high force densities and efficiencies, making the use of a PM LSM ideal for the GES system. Conventional PM LSMs, which have magnets placed on the secondary, have received attention for use in ropeless elevators, i.e. long secondary applications, due to their inherently large force density [79,62–64] with novel dual-PM linear motors developed in [61]. These topologies are not considered, do to the placement of PMs on the secondary.

LMs in the variable reluctance permanent magnet (VRPM) family allow for higher σ values to be achieved. The transverse flux machine (TFM) can reach shear stress values up to 200 kN/m² [74], however, due to the non-conventional machine structure and the associated construction difficulties, this topology is not suited for the GES system application. The linear vernier hybrid (VH) permanent magnet machine, which is a variant of a normal vernier machine with the magnets placed on the stator [80], has been noted to reach shear stress values up to 143.9 kN/m² [81], though the VHPM is notorious for its low power factor, which increases the cost of the power electronics needed to drive it. Another option is the linear flux-switching permanent magnet and flux-switching wound field machines, where all the active material is on the primary. They generally have higher shear stress than conventional PM machines [68,60].

Other PM-less LM options, in the linear reluctance machine family, with high shear stress values are the linear switched reluctance machines (LSRMs), with σ values up to 35 kN/m² [82], and the flux-controllable variable reluctance machine, with σ values up to 50 kN/m² [83].

6.4. Hoisting capability and practical implementation

The ideal shape for the LM is tubular, as that ensures maximum air gap area. However, taking into account the placement of the brakes, power supply and guideway, the tubular shape is difficult to construct practically and as such the more practical four-sided LM shape is used to demonstrate the hoisting capability.

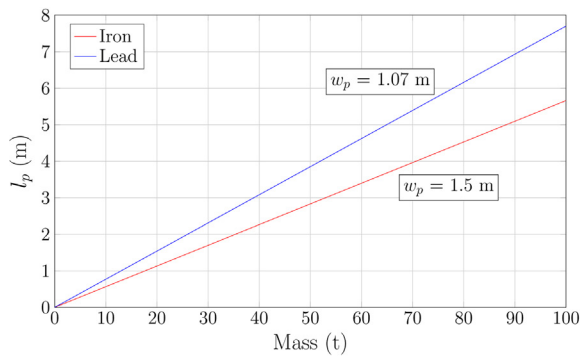
Using the four-sided shape and choosing two shear stress values, 30 and 100 kN/m², based on the preceding overview, the width of an LM-based piston is determined for two different piston materials identified in Section 4. The results are shown in Table 10.

Using this piston width and the two material choices, the piston length as the mass is increased is shown in Fig. 18. This demonstrates that a higher density material produces a narrower and longer piston. The achievable 30 kN/m² shear stress can provide hoisting capability that is very similar to the four-drum wire rope hoist discussed in Section 5, and when considering the same piston volume of 14 m³ of that system, an iron-based LM piston would be able to hoist slightly more than 100 t, with a piston length of 6 m. For the same piston, but assuming a σ value of 100, the piston length would only be 0.5 m.

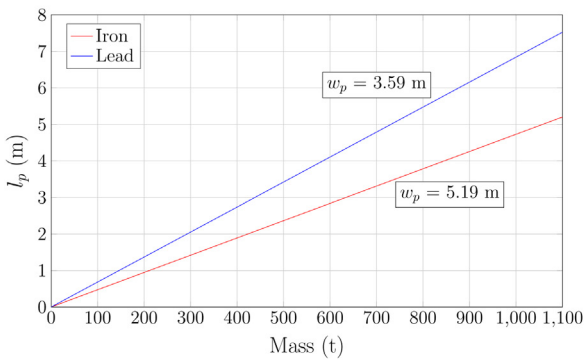
While it appears that the LM offers the same kind of hoisting capacity as the wire rope hoist, it provides extra modularity. Since there are no wire ropes and no active material on the secondary, it is possible to have a GES system with one shaft and multiple pistons as shown in Fig. 19. This allows for more efficient use of the passive secondary that has to be installed in the shaft as well as enormously increase the amount of mass that can be hoisted, and thus the storage capacity, while allowing the active primary of the LM to be sized based on

Table 10
Minimum width requirements.

Material	$\sigma = 30 \text{ kN/m}^2$	$\sigma = 100 \text{ kN/m}^2$
	w_p	w_p
Iron	1.5 m	5.19 m
Lead	1.07 m	3.59 m



(a) Mass versus piston length for a shear stress of 30 kN/m².



(b) Mass versus piston length for a shear stress of 100 kN/m².

Fig. 18. The piston mass vs piston length for the two shear stress values.

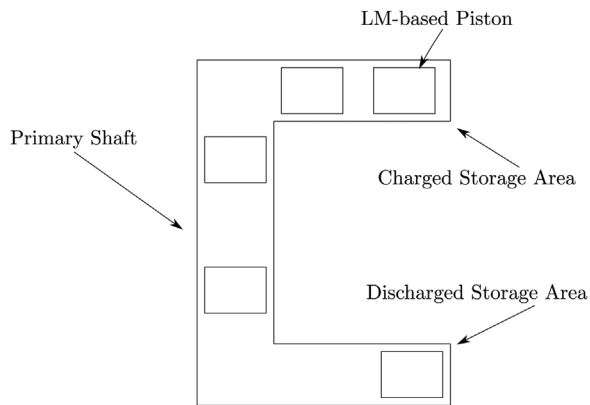


Fig. 19. A simple multi-piston implementation of a LM-based GES system.

practical considerations instead of designing for maximum possible hoisting weight. This can work especially well in underground systems, such as mine shafts, as there is already space for both the charged and discharged store areas.

As an example, consider a four-sided iron-based piston, with a LM length of 3 m and a shear stress of 30 kN/m². This gives a piston mass of 50 t. At a 100 m system height, from Fig. 12, a wire rope hoist can realistically be expected to hoist 200 t. Using LMs at the same height theoretically allows for up to 30 pistons in the shaft at one time, making an effective 1500 t of piston mass and 90 m piston length.

This difference becomes even more pronounced when considering a system height of 2000 m, with the wire rope system being able to hoist around 110 t. At this height, the shaft could fit up to 665 3 m pistons at once, to produce a total effective piston mass of 33 250 t and effective piston length of 1995 m. Some specifications of these two systems, assuming a discharge of 0.5 h, is given in Table 11.

Table 11
Specifications of two iron-based LM GES system.

h (m)	Number of pistons	Energy storage (kWh)	Energy density (kWh/m ³)	Power density (kW/m ³)
100	30	408	1.926	3.85
2000	665	181 200	42.7	85.4

The values given for these two systems do assume that the shafts are the same width as the pistons, which would not likely be the case in a real world application. This means that the energy and power density would be lower for the actual implementation, although still significantly higher than would be achievable in the wire rope system.

Similarly, the discharge time of 0.5 h is assumed to allow the power density to be readily comparable to the wire rope systems in Section 5, and the amount of pistons are chosen to demonstrate a maximum theoretical value. It is likely that these choices would not be optimal for the LM hoist, as all the pistons will only be in the shaft simultaneously for a very short time, during which the power supply would need to handle a very large amount of current.

A more likely use case would be to design a system that discharges over a long time, thereby bringing the power requirement down, e.g. from 362 MW for a 30 min discharge to 22.625 MW for an 8 h discharge time over 2000 m. An 8 h discharge time would effectively mean that only 83 of the 665 pistons would be in the shaft at the same time, thus reducing the energy and power density values given in Table 11, while still keeping the same number of total pistons and energy storage capacity. A system like this would also only be limited by the storage space for the pistons, thus enabling even longer discharge times without altering the initial LM design.

The LM-based GES thus extends the capability of the GES beyond that which can be achieved through wire rope hoisting by enabling very long discharge times, e.g. 8 h versus the 0.5 h of a drum winder hoist, and large energy storage capacities, e.g. 180 MWh versus the 600 kWh of a drum winder hoist.

6.5. Discussion

The LM-based GES system proposed in this section possesses a lot of potential. It can dramatically increase the storage capacity above that of the wire rope system and provides further flexibility in maintenance, as each piston can be removed and replaced separately, without a significant effect on the overall performance of the GES system. This method also offers a certain amount of adaptability, as pistons can be added to extend the storage capacity at any time, as well as allowing the introduction of improved primary designs throughout the system's lifetime. This also allows for the use of smaller pistons, making them easier to manufacture and install.

However, this system also has a lot of challenges. Adequately designing an LM with a proper braking system will be challenging, while proper control for such a GES system is likely to be complex. Multi-car elevator systems have received some research attention [84–86,69,87] and Thyssenkrupp is working on a commercial version of this concept, but this is still a new technology. Designing and operating the movement into and out of the storage areas will be challenging. Having multiple pistons in a single shaft also increases the response time of the storage system, as it will take longer to reach full power output. The cost of installing a secondary of these lengths, as well as the multiple primaries also needs to be further researched and considered. The likely increase in discharge time also affects the LCOS of the GES, as this limits the achievable annual cycles. However, the maintenance cost should be less, especially if an electromagnetic guideway and contactless power supply is used. Similarly, the replacement cost would be significantly less, as there are no wire ropes, drum winders or gearboxes that would need replacing. The downtime for any maintenance or

replacement of the primaries should also be negligible, as a single primary can be removed without affecting the storage system significantly.

Regardless of the economic and technological challenges, the LM-based system remains an attractive variant of the GES system, offering more versatility than the wire rope system and making large storage capacities achievable, at the expense of increased response time and system complexity.

7. Conclusion

A gravity-based energy storage method, the GES system, is introduced, analysed and discussed in this paper. The GES is a waterless, electromechanical form of energy storage, with less stringent geographical requirements than traditional PHES.

The modelling of the GES system is done in Section 3, providing equations for the storage capacity, energy and power density. In the following section, the performance of the GES, disregarding the hoisting method, is discussed. This section gives concrete values for the storage capacity, energy and power densities that can easily be used to compare with other storage technologies. It also provides a look at the optimal discharge time. This shows that the GES is most likely to compete with flow batteries, as it has similar power and energy densities and thus will have similar applications. A brief LCOS is also done, with different piston material being considered, showing that iron and lead are viable choices. This also shows that higher annual cycles will likely be the best way to keep the GES economically competitive. Sensitivity analyses are done with regards to the CAPEX, COPEX, CAPEX_{res}, η , cost of input electrical energy and recovery value. The CAPEX_{re} has the largest effect on the estimated LCOS, alongside the recovery value. However, the LCOS evaluation is limited, as it did not include any hoisting specific costs. As such, further research is needed to determine the exact costs of the different hoisting methods.

Two different hoisting methods are then proposed. The first one is the traditional drum winder hoist, similar to the ones used in mine, elevator and ship hoists. Only commercially available options are reviewed, to demonstrate the limiting effect that the use of wire rope has on the piston mass and therefore the storage capacity of the GES. The hoist, while offering limited storage capacity with commercially available wire ropes, can be improved upon by specially designed and built options. The advantage of this hoisting method is the maturity of winder drum systems, which could likely result in a less costly system and more readily available expertise. The wire rope system also provides the flexibility of being able to be deployed in most conditions, enabling offshore installations, as proposed by MGH. The most likely use case of a GES system with a drum winder hoist will be for high power applications with high annual charge/discharge cycles, thus taking advantage of the theoretically limitless cyclability and fast response times.

The second method introduced the concept of a linear electric machine as hoist. Different subcomponents, such as the power supply, guideways and brakes, are briefly discussed by drawing from various other industries and applications. Finally, using the advantage of ropeless operation, a multi-piston GES is suggested. This greatly increases the storage capacity, while simultaneously keeping the piston size small and easily manufacturable and also provides more design freedom and flexibility. This comes at the cost of using technology that is still in the concept phase, which could increase the overall system cost. The additional storage capacity and the longer discharge times, the use case for a LM-based GES is likely to be in the form of bulk energy storage, performing task such as load shifting and longer term storage.

The GES is a feasible and promising storage technology, but still requires further research to develop some of the components, enabling a more detailed comparison to existing storage technologies.

References

- [1] P.D. Lund, J. Lindgren, J. Mikkola, J. Salpakari, Review of energy system flexibility measures to enable high levels of variable renewable electricity, *Renew. Sustain. Energy Rev.* 45 (2015) 785–807, <https://doi.org/10.1016/j.rser.2015.01.057>.
- [2] E.A. Bakirtzis, C.K. Simoglou, P.N. Biskas, A.G. Bakirtzis, Storage management by rolling stochastic unit commitment for high renewable energy penetration, *Electric Power Syst. Res.* 158 (2018) 240–249, <https://doi.org/10.1016/j.epsr.2017.12.025>.
- [3] P. Denholm, M. Hand, Grid flexibility and storage required to achieve very high penetration of variable renewable electricity, *Energy Policy* 39 (2011) 1817–1830, <https://doi.org/10.1016/j.enpol.2011.01.019>.
- [4] R. Adib, H.E. Murdock, Highlights of the REN21 Renewables 2017 Global Status Report in Perspective, (2017) URL: http://www.ren21.net/wp-content/uploads/2017/06/GSR2017_Highlights_FINAL.pdf.
- [5] M. McPherson, S. Tahseen, Deploying storage assets to facilitate variable renewable energy integration: the impacts of grid flexibility, renewable penetration, and market structure, *Energy* (2018), <https://doi.org/10.1016/j.energy.2018.01.002>.
- [6] T.M. Letcher, *Storing Energy: With Special Reference to Renewable Energy Sources*, (2016).
- [7] M. Aneke, M. Wang, Energy storage technologies and real life applications – a state of the art review, *Appl. Energy* 179 (2016) 350–377, <https://doi.org/10.1016/j.apenergy.2016.06.097>.
- [8] A. Castillo, D.F. Gayme, Grid-scale energy storage applications in renewable energy integration: a survey, *Energy Convers. Manage.* 87 (2014) 885–894, <https://doi.org/10.1016/j.enconman.2014.07.063>.
- [9] M.S. Guney, Y. Tepe, Classification and assessment of energy storage systems, *Renew. Sustain. Energy Rev.* 75 (2017) 1187–1197, <https://doi.org/10.1016/j.rser.2016.11.102>.
- [10] Y. Hou, R. Vidu, P. Stroeve, Solar energy storage methods, *Ind. Eng. Chem. Res.* 50 (2011) 8954–8964, <https://doi.org/10.1021/ie2003413>.
- [11] W.F. Pickard, The history, present state, and future prospects of underground pumped hydro for massive energy storage, *Proc. IEEE* 100 (2012) 473–483, <https://doi.org/10.1109/JPROC.2011.2126030>.
- [12] D. Rastler, *Electricity Energy Storage Technology Options: A White Paper Primer on Applications, Costs and Benefits*, Electric Power Research Institute, 2010.
- [13] S.O. Amrouche, D. Rekioua, T. Rekioua, S. Bacha, Overview of energy storage in renewable energy systems, *Int. J. Hydrogen Energy* 41 (2016) 20914–20927, <https://doi.org/10.1016/j.ijhydene.2016.06.243>.
- [14] G. Locatelli, E. Palerma, M. Mancini, Assessing the economics of large energy storage plants with an optimisation methodology, *Energy* 83 (2015) 15–28, <https://doi.org/10.1016/j.energy.2015.01.050>.
- [15] T. Mahlia, T. Saktisahdan, A. Jannifar, M. Hasan, H. Matseelar, A review of available methods and development on energy storage; technology update, *Renew. Sustain. Energy Rev.* 33 (2014) 532–545, <https://doi.org/10.1016/j.rser.2014.01.068>.
- [16] B. Zakeri, S. Syri, Electrical energy storage systems: a comparative life cycle cost analysis, *Renew. Sustain. Energy Rev.* 42 (2015) 569–596, <https://doi.org/10.1016/j.rser.2014.10.011>.
- [17] S. Rehman, L.M. Al-Hadhrami, M.M. Alam, Pumped hydro energy storage system: a technological review, *Renew. Sustain. Energy Rev.* 44 (2015) 586–598, <https://doi.org/10.1016/j.rser.2014.12.040>.
- [18] E. Pujades, T. Willems, S. Bodeux, P. Orban, A. Dassargues, Underground pumped storage hydroelectricity using abandoned works (deep mines or open pits) and the impact on groundwater flow, *Hydrogeol. J.* 24 (2016) 1531–1546, <https://doi.org/10.1007/s10040-016-1413-z>.
- [19] F. Winde, F. Kaiser, E. Erasmus, Exploring the use of deep level gold mines in South Africa for underground pumped hydroelectric energy storage schemes, *Renew. Sustain. Energy Rev.* 78 (2017) 668–682, <https://doi.org/10.1016/j.rser.2017.04.116>.
- [20] Gravity Power – Grid Scale Energy Storage, [Online]. Available: <http://www.gravitypower.net/> (accessed: February 2018).
- [21] Heindl Energy Storage [Online]. Available: <https://heindl-energy.com> (accessed: February 2018).
- [22] Escovale Consultancy Services [Online]. Available: <http://www.escovale.com/GBES.php> (accessed: February 2018).
- [23] labeleda A. Berrada, K. Loudiyi, I. Zorkani, System design and economic performance of gravity energy storage, *J. Clean. Prod.* 156 (2017) 317–326, <https://doi.org/10.1016/j.jclepro.2017.04.043>.
- [24] A. Berrada, K. Loudiyi, I. Zorkani, Dynamic modeling and design considerations for gravity energy storage, *J. Clean. Prod.* 159 (2017) 336–345.
- [25] E. Heindl, Hydraulic hydro storage system for self-sufficient cities, *Energy Procedia* 46 (2014) 98–103, <https://doi.org/10.1016/j.egypro.2014.01.162>.
- [26] F. Escombe, GBES – Ground-Breaking Energy Storage (GBES-01), Available: <http://www.escovale.com/downloads/GBES-01-Introduction.pdf>.
- [27] R. Cazzaniga, M. Cicu, T. Marrana, M. Rosa-Clot, P. Rosa-Clot, G. Tina, Doges: deep ocean gravitational energy storage, *J. Energy Storage* 14 (2017) 264–270, <https://doi.org/10.1016/j.est.2017.06.008>.
- [28] A.H. Slocum, G.E. Fennell, G. Dundar, B.G. Hodder, J.D. Meredith, M.A. Sager, Ocean renewable energy storage (ores) system: analysis of an undersea energy storage concept, *Inst. Electr. Electron. Eng.* (2013), <https://doi.org/10.1109/JPROC.2013.2242411>.
- [29] Ares – The Power of Gravity [Online]. Available: <https://www.aresnorthamerica.com/> (accessed 2018).
- [30] Gravitricity [Online]. Available: <https://www.gravitricity.com/> (accessed: March 2018).

- [31] C. Blair, Gravitricity – Storing Power as well as Energy [Online]. Available: <http://www.all-energy.co.uk/Conference/Download-2016-Presentations/>.
- [32] B. Bungane, Gravitricity Sets Sights on South Africa to Test Green Energy Tech [Online]. Available: <https://www.esi-africa.com/gravitricity-sets-sights-south-africa-test-green-energy-tech/> (accessed: March 2018).
- [33] Gravitricity Teams up with Worldwide Lifting, Drilling and Subsea Specialists Huisman to Build Prototype Energy Store [Online]. Available: <https://www.huismanequipment.com/> (accessed: March 2018).
- [34] MGH – Deep Sea Energy Storage [Online]. Available: <http://www.mgh-energy.com/> (accessed: August 2018).
- [35] Stratosolar [Online]. Available: <http://www.stratosolar.com/> (accessed: August 2018).
- [36] T. Mushiri, M. Jirivengwa, C. Mbohwa, Design of a hoisting system for a small scale mine, *Procedia Manuf.* 8 (2017) 738–745, <https://doi.org/10.1016/j.promfg.2017.02.095>.
- [37] Guideline for Design, Commissioning and Maintenance of Drum Winders. 1998.
- [38] V. Jülch, Comparison of electricity storage options using leveled cost of storage (LCOS) method, *Appl. Energy* 183 (2016) 1594–1606, <https://doi.org/10.1016/j.apenergy.2016.08.165>.
- [39] J.A. Ober, Mineral Commodity Summaries 2018, Technical Report, US Geological Survey, 2018.
- [40] Metalary [Online]. Available: <https://www.metalary.com> (last accessed: September 2018).
- [41] P. Nikolaidis, A. Poullikas, Cost metrics of electrical energy storage technologies in potential power system operations, *Sustain. Energy Technol. Assess.* 25 (2018) 43–59, <https://doi.org/10.1016/j.seta.2017.12.001>.
- [42] A. McKane, A. Hasanbeigi, Motor systems energy efficiency supply curves: a methodology for assessing the energy efficiency potential of industrial motor systems, *Energy Policy* 39 (2011) 6595–6607, <https://doi.org/10.1016/j.enpol.2011.08.004>.
- [43] L.J. Fingersh, M.M. Hand, A.S. Laxson, *Wind Turbine Design Cost and Scaling Model*, (2006).
- [44] O. Schmidt, Levelised Cost of Storage for Gravitricity Storage Systems, Available on request from: charlie.blair@gravitricity.com.
- [45] P. Darling, *SME Mining Engineering Handbook vol. 1*, SME, 2011.
- [46] P. McCarthy, R. Livingstone, Shaft or decline? An economic comparison, *Open Pit to Underground: Making the Transition* AIG Bulletin, (1993), pp. 45–56.
- [47] P.R. Childs, *Mechanical Design Engineering Handbook*, Elsevier, 2014.
- [48] J.E. Shigley, *Shigley's Mechanical Engineering Design*, Tata McGraw-Hill Education, 2011.
- [49] L. Bronn, R. Wang, M. Kamper, Development of a shutter type magnetic gear, in: *Proceedings of the 19th Southern African Universities Power Engineering Conference* (2010) 78–82.
- [50] K. Nakamura, M. Fukuoka, O. Ichinokura, Performance improvement of magnetic gear and efficiency comparison with conventional mechanical gear, *J. Appl. Phys.* 115 (2014) 17A314, <https://doi.org/10.1063/1.4863809>.
- [51] Magnomatics – Magnetically Geared. URL: <http://www.magnomatics.com/pages/technology/innovation.htm>.
- [52] P. Tlali, R. Wang, S. Gerber, Magnetic gear technologies: a review, 2014 International Conference on Electrical Machines (ICEM), IEEE, 2014, pp. 544–550, <https://doi.org/10.1109/ICELMACH.2014.6960233>.
- [53] J. Rens, K. Atallah, S.D. Calverley, D. Howe, A novel magnetic harmonic gear, *IEEE Trans. Ind. Appl.* 46 (2010) 206–212, <https://doi.org/10.1109/ICELMACH.2008.4800163>.
- [54] G. Zhou, X. Xu, Y. Xiong, L. Zhang, Design and analysis of low-speed high torque direct-driven permanent magnet synchronous machines (PMSM) with fractional-slot concentrated winding used in coal mine belt conveyor system, 2017 20th International Conference on Electrical Machines and Systems (ICEMS), IEEE, 2017, pp. 1–5, <https://doi.org/10.1109/ICEMS.2017.8056054>.
- [55] K. Atallah, S. Calverley, R. Clark, J. Rens, D. Howe, A new pm machine topology for low-speed, high-torque drives, 18th International Conference on Electrical Machines, ICEM 2008, IEEE, 2008, pp. 1–4, <https://doi.org/10.1109/ICELMACH.2008.4799909>.
- [56] D. Powell, S. Calverley, F. De Wildt, K. Daffey, Design and Analysis of a Pseudo Direct-Drive Propulsion Motor, (2010), <https://doi.org/10.1049/cp.2010.0025>.
- [57] I. Boldea, L.N. Tutelea, W. Xu, M. Pucci, Linear electric machines, drives, and maglevs: an overview, *IEEE Trans. Ind. Electron.* 65 (2018) 7504–7515, <https://doi.org/10.1109/TIE.2017.2733492>.
- [58] Q. Lu, W. Mei, Recent development of linear machine topologies and applications, *CES Trans. Electr. Mach. Syst.* 2 (2018) 65–72, <https://doi.org/10.23919/TEMS.2018.8326452>.
- [59] J.F. Gieras, Z.J. Piech, B. Tomczuk, *Linear Synchronous Motors: Transportation and Automation Systems*, CRC Press, 2016.
- [60] J. Faiz, A. Nematsaberi, Linear electrical generator topologies for direct-drive marine wave energy conversion – an overview, *IET Renew. Power Gener.* 11 (2017) 1163–1176, <https://doi.org/10.1049/iet-rpg.2016.0726>.
- [61] H. Fan, K. Chau, C. Liu, L. Cao, T. Ching, Quantitative comparison of novel dual-PM linear motors for ropeless elevator system, *IEEE Trans. Magn.* (2018) 1–6, <https://doi.org/10.1109/TMAG.2018.2842083>.
- [62] S.-G. Lee, S.-A. Kim, S. Saha, Y.-W. Zhu, Y.-H. Cho, Optimal structure design for minimizing detent force of PMLSM for a ropeless elevator, *IEEE Trans. Magn.* 50 (2014) 1–4, <https://doi.org/10.1109/TMAG.2013.2277544>.
- [63] Q. Lu, Y. Yao, Y. Ye, J. Dong, Research on ropeless elevator driven by PMLSM, 2016 Eleventh International Conference on Ecological Vehicles and Renewable Energies (EVER), IEEE, 2016, pp. 1–6, <https://doi.org/10.1109/EVER.2016.7476386>.
- [64] Y.-w. Zhu, S.-g. Lee, Y.-h. Cho, Topology structure selection of permanent magnet linear synchronous motor for ropeless elevator system, 2010 IEEE International Symposium on Industrial Electronics (ISIE), IEEE, 2010, pp. 1523–1528, <https://doi.org/10.1109/ISIE.2010.5637992>.
- [65] R. Appunn, K. Hameyer, Modern high speed elevator systems for skyscrapers, *Maglev-2014, Rio de Janeiro, Brazil*, 2014, p. 24.
- [66] H.S. Lim, R. Krishnan, N.S. Lobo, Design and control of a linear propulsion system for an elevator using linear switched reluctance motor drives, *IEEE Trans. Ind. Electron.* 55 (2008) 534–542, <https://doi.org/10.1109/TIE.2007.911942>.
- [67] H.S. Lim, R. Krishnan, Ropeless elevator with linear switched reluctance motor drive actuation systems, *IEEE Trans. Ind. Electron.* 54 (2007) 2209–2218, <https://doi.org/10.1109/TIE.2007.899875>.
- [68] B. Zhang, M. Cheng, S. Zhu, M. Zhang, W. Hua, R. Cao, Investigation of linear flux-switching permanent magnet machine for ropeless elevator, 2016 19th International Conference on Electrical Machines and Systems (ICEMS), IEEE, 2016, pp. 1–5.
- [69] Ç. GÜRBÜZ, E. Kazan, A. Onat, S. Markon, Linear motor for multi-car elevators: design and position measurement, *Turk. J. Electr. Eng. Comput. Sci.* 19 (2011) 827–838.
- [70] J. Loeb, Real-life 'wonkavator' could revolutionise design of skyscrapers [news briefing], *Eng. Technol.* 12 (2017) 10–11.
- [71] R. Appunn, B. Riemer, K. Hameyer, Contactless power supply for magnetically levitated elevator systems, 2012 XXth International Conference on Electrical Machines (ICEM), IEEE, 2012, pp. 600–605, <https://doi.org/10.1109/ECCE.2010.5618232>.
- [72] B. Schmölling, P. Laumen, K. Hameyer, Improvement of a non-contact elevator guiding system by implementation of an additional torsion controller, 2010 IEEE on Energy Conversion Congress and Exposition (ECCE), IEEE, 2010, pp. 2971–2976, <https://doi.org/10.1109/ECCE.2010.5618232>.
- [73] S.Y. Choi, B.W. Gu, S.Y. Jeong, C.T. Rim, Advances in wireless power transfer systems for roadway-powered electric vehicles, *IEEE J. Emerg. Select. Top. Power Electron.* 3 (2015) 18–36, <https://doi.org/10.1109/JESTPE.2014.2343674>.
- [74] M. Mueller, H. Polinder, N. Baker, Current and novel electrical generator technology for wave energy converters, IEEE International on Electric Machines & Drives Conference 2007, IEMDC'07, vol. 2, IEEE, 2007, pp. 1401–1406.
- [75] H. Polinder, B.C. Mecrow, A.G. Jack, P.G. Dickinson, M.A. Mueller, Conventional and TFPM linear generators for direct-drive wave energy conversion, *IEEE Trans. Energy Convers.* 20 (2005) 260–267.
- [76] R.J. Cruise, C.F. Landy, Linear synchronous motor propelled hoists for mining applications, Conference Record of the 1996 IEEE on Industry Applications Conference, Thirty-First IAS Annual Meeting, IAS'96, vol. 4, IEEE, 1996, pp. 2514–2519.
- [77] C.F. Landy, R.J. Cruise, Design considerations of linear motor hoists for underground mining operations, South African Universities Power Engineering Conference 1998, vol. 4 (1998) 65–68.
- [78] R.J. Cruise, C.F. Landy, Linear synchronous motor hoisting systems for ultra-deep level mining, South African Universities Power Engineering Conference 1999, vol. 4 (1999) 106–109.
- [79] H. Fan, K. Chau, C. Liu, Z. Zhang, C. Qiu, Quantitative comparison of permanent magnet linear machines for ropeless elevator, IECN 2015-41st Annual Conference of the IEEE on Industrial Electronics Society, IEEE, 2015, pp. 005357–005362, <https://doi.org/10.1109/IECON.2015.7392945>.
- [80] E. Spooner, L. Haydock, Vernier hybrid machines, *IEE Proc. Electr. Power Appl.* 150 (2003) 655–662.
- [81] M. Mueller, N. Baker, A Low Speed Reciprocating Permanent Magnet Generator for Direct Drive Wave Energy Converters, (2002).
- [82] J. Du, D. Liang, L. Xu, Q. Li, Modeling of a linear switched reluctance machine and drive for wave energy conversion using matrix and tensor approach, *IEEE Trans. Magn.* 46 (2010) 1334–1337, <https://doi.org/10.1109/TMAG.2010.2041041>.
- [83] W. Li, K. Chau, C. Liu, C. Qiu, Design and analysis of a flux-controllable linear variable reluctance machine, *IEEE Trans. Appl. Supercond.* 24 (2014) 1–4, <https://doi.org/10.1109/TASC.2013.2284720>.
- [84] S. Chevaillier, M. Jufer, Y. Perriard, T. Duenser, H. Kocher, Linear motors for multi mobile systems, Conference Record of the 2005 on Industry Applications Conference, Fortieth IAS Annual Meeting, vol. 3, IEEE, 2005, pp. 2099–2106.
- [85] A. Cassat, B. Kawkabani, Y. Perriard, J.-J. Simond, Power supply of long stator linear motors – application to multi mobile system, Industry Applications Society Annual Meeting, IAS'08, IEEE, 2008, pp. 1–7.
- [86] A. Onat, E. Kazan, N. Takahashi, D. Miyagi, Y. Komatsu, S. Markon, Design and implementation of a linear motor for multicar elevators, *IEEE/ASME Trans. Mechatron.* 15 (2010) 685–693.
- [87] N. Takahashi, T. Yamada, D. Miyagi, S. Markon, Basic Study of Optimal Design of Linear Motor for Rope-Less Elevator, (2008).